Mathematical modeling of seasonal epidemics: an analysis of influenza and COVID-19 transmission dynamics and vaccine intervention timing

Jinchi Cui

Supervisors
Professor Kathryn Glass
National Centre for Epidemiology & Population Health
Associate Professor Pierre Portal
Mathematical Sciences Institute

October 2024

A thesis submitted for the degree of Master in Mathematical Sciences (Advanced) of the Australian National University

Australian National University

For all those who have suffered during the COIVD-19 pandemic

Declaration

The work in this thesis is my own except where otherwise stated.

Jinchi Cui

Acknowledgements

First and foremost, I would like to express my sincere gratitude to my supervisors, Professor Kathryn Glass and Associate Professor Pierre Portal, for their patient guidance, without which I would not have been able to complete this thesis. I also want to thank my parents, whose unconditional support, both emotionally and financially, has provided me the opportunity to pursue my graduate studies in Australia. Additionally, during my time at the Australian National University, I met my wife, to whom I am deeply grateful for her suggestions on the structure and wording of this thesis, as well as for her support in both my personal life and mental well-being.

As a mathematics student, many of us often contemplate the significance of mathematics in our lives, and the answer is different for everyone. People often stereotype those working in mathematics as rational but emotionally detached. However, it is precisely the question of the meaning of mathematics that speaks to the more emotional side of our nature. Since I began my studies in mathematics in 2019 and now approach the end of my graduate studies in 2024, I have been in constant pursuit of applying what I've learned to practical situations.

I completed my undergraduate studies at Shandong University in China, and I will never forget the first two years of my university life. Due to the outbreak of COVID-19, strict lockdown policies meant that students were unable to freely enter and leave campus or attend classes in person. During that time, I often felt a deep sense of helplessness, questioning whether the knowledge I was acquiring could make any real impact when faced with the harsh realities of life and death. However, this research project has given me the chance to contribute, however modestly, to society.

Though this is not my first mathematical modeling project—I had previously worked on research related to consumer equilibrium models and the cobweb model for pork prices—it is the first time I truly felt that I was making a tangible contribution to the well-being of others. My father is a doctor, and my mother

also works in the medical field. Growing up in such a family has instilled in me a deep sense of empathy and responsibility toward those suffering from illness. Therefore, I am especially fortunate to have had the opportunity to work on an interdisciplinary project involving both mathematics and epidemiology at the Australian National University, despite epidemiology being a field unfamiliar to me.

I will always cherish the time I spent in Canberra. Here, I found not only esteemed mentors and great friends, but also my life partner, and I have come to better understand the personal significance of mathematics in my life. Words may be limited, but my gratitude is boundless. Thank you.

Abstract

This study, assuming a certain level of seasonality for COVID-19, develops an age-structured ordinary differential equation (ODE) model to simulate the transmission dynamics of influenza and COVID-19, as well as the impact of different vaccination timing on epidemic control. Additionally, the principles of the next-generation matrix method are discussed, along with the relationship between the basic reproduction number and the asymptotic stability of the ODE model. The results suggest that promoting the simultaneous vaccination of influenza and COVID-19 can have a positive effect in reducing the total number of infections.

Contents

Notation and terminology

NGM	Next generation matrix
NNDSS	National Notifiable Diseases Surveillance System
LFD	Linear feasible direction
SEIRV	Susceptible, Exposed, Infected, Removed, Vaccinated
R_0	Basic reproduction number
DFE	Disease free equilibrium
ODE	Ordinary differential equations
PDE	Partial differential equations

Chapter 1

Introduction

1.1 Seasonality of COVID-19 and influenza

Since the outbreak of the COVID-19 pandemic in 2019, preventive measures for this disease have gradually transitioned into a state of normalization. This shift means that scholars are paying more attention to the long-term transmission patterns of COVID-19. Research by Liu et al.[8] points out that 40% to 60% of COVID-19 cases are related to seasonality. Similarly, Mohammad et al.'s research [13] suggests that large-scale community outbreaks of COVID-19 follow a distribution along latitude, temperature, and humidity, consistent with the behavior of seasonal respiratory viruses. These characteristics suggest similarities between the transmission patterns of COVID-19 and the seasonal spread of influenza. Wei's[15] analysis of influenza seasonality shows that influenza cases exhibit strong periodicity in all regions globally. Therefore, it is worth considering the introduction of seasonal factors into COVID-19 models in epidemiological modeling to achieve more accurate simulations.

Jeffrey et al[16]. pointed out that "the timing and pattern of potential seasonal surges remain uncertain, making public health policy uninformed and possibly missing intervention opportunities, such as timely booster vaccinations." This uncertainty is due to the fact that, since the outbreak of COVID-19 in 2019, human interventions such as isolation measures and vaccines have disrupted the natural development of herd immunity, meaning that the virus has not yet entered a state of dynamic equilibrium. As a result, it is challenging to estimate seasonal parameters effectively from existing data. However, since COVID-19 is likely to follow a similar transmission trend as influenza, it is of research significance to consider adopting similar vaccination interventions.

We propose that aligning the availability of the COVID-19 vaccine with the availability of the influenza vaccine could effectively encourage the public to receive both vaccines simultaneously. However, due to the influence of seasonality, the peak incidence times of influenza and COVID-19 do not necessarily coincide, and the coverage and effectiveness of the two vaccines vary across different age groups. Therefore, simultaneous vaccination could potentially reduce the protective effect. Thus, we aim to establish an epidemic model with age structure and seasonal characteristics to simulate the impact of different vaccine availability periods on epidemic control, thereby verifying the feasibility of this approach.

1.2 Outline of the thesis

In this thesis, we build a mathematical model of influenza and COVID-19 transmission, in order to inform control measures for both diseases. Specifically, the goals of this thesis are as follows:

1. Discuss the mathematical definition and dynamic analysis of generalized epidemic models, and describe seasonal models. Prove the existence and uniqueness of solutions to the SEIRS system.

2. Provide an overview of the concept of basic reproduction numbers, restating the principles of the next-generation matrix method, and relate them to the stability of epidemic models.

3. Extend the model by introducing vaccines and presenting numerical solutions.

4. Use seasonal influenza as an example to estimate the parameters of the SEIRVS model, and discuss the principles of L-1 and L-2 regularization.

5. Incorporate age structure into the model and analyze the impact of different vaccine intervention times on the total number of infections of influenza and COVID-19.

Chapter 2

Disease transmission model overview

2.1 Definition of a disease transmission model

A disease transmission model is a well-built mathematical model used to describe and predict the dynamics of an infectious disease such as COVID-19, SARS, etc. These models are often described by a system of ordinary differential equations (ODEs) as a function of the time variable. We are going to define the model mathematically.

Definition 1: The total population at a given time is divided into compartments such that all individuals in the compartment have the same infectious status at that time in the epidemic outbreak. These compartments often include:

- **Susceptible:** individuals that could be infected by the disease.
- **Infected:** individuals that are infected with the disease.
- **Removed:** individuals that are removed from the system (usually recovered and immune or dead).

2.1.1 Simple case: The SIRS model

In 1991, the Kermack–McKendrick theory was re-published[7] to provide a solid foundation for the disease transmission model. A well-known simple case of the disease transmission model is the SIRS model.

In a classic SIR disease transmission model, the population inside the "Removed" compartment will not leave that compartment. However, in reality, immunity that people get after recovering from the disease is not always life-long. Thus, it is important to introduce an additional flow from the "Removed" group to the "Susceptible" group to model waning immunity.

Model set up

Assumptions:

- The total population is fixed.
- The model does not consider births and deaths.

Definition 2: Define compartments in this model ("Susceptible","Infectious","Recovered") as functions in C^1

- $S(t) : \mathbb{R}^+ \to \mathbb{R}^+$
- $I(t) : \mathbb{R}^+ \to \mathbb{R}^+$
- $R(t) : \mathbb{R}^+ \to \mathbb{R}^+$

We now introduce $\beta \in [0, +\infty)$, a parameter that represents the transmission rate between individuals and determines the flow between the "Susceptible" group and the "Infectious" group. In this model, we describe the contact between susceptible and infectious individuals as the product of the number of people in group S and group I. This product (contact) multiplied by beta (effective contact rate) is used to describe the infection rate. We define $\delta \in \mathbb{R}^+$ as the rate of loss of immunity : $\delta = \frac{1}{\text{duration-of-immunity}}$. Similarly, γ is the recovery rate $\gamma = \frac{1}{\text{infectious-period}}$

The process of the SIRS model is shown in Figure 2.1, where the solid lines indicate flows of people and the dotted line indicates the infection path.
While N is represent the total population, the model shown in Figure 1.1 is described by the following ODE system:

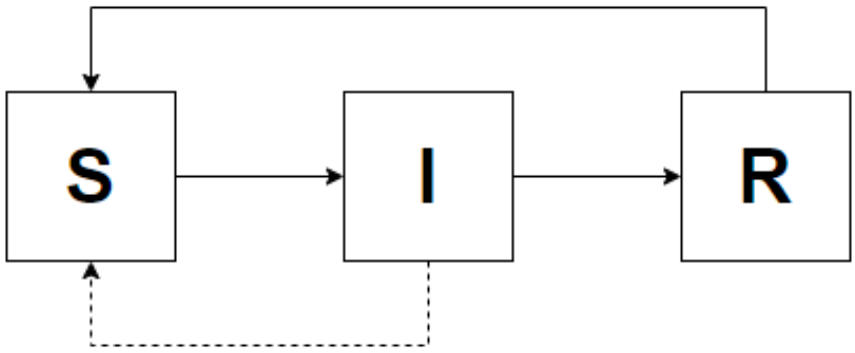

Figure 2.1: SIR process diagram. Solid lines show movement of people and dotted lines indicate infection paths.

$$\begin{cases} \frac{dS}{dt} = -\frac{\beta SI}{N} + \delta R \\ \frac{dI}{dt} = \frac{\beta SI}{N} - \gamma I \\ \frac{dR}{dt} = \gamma I - \delta R \\ S(0) = s_0, \quad s_0 \in \mathbb{R}^+ \\ I(0) = i_0, \quad i_0 \in \mathbb{R}^+ \\ s_0 + i_0 + r_0 = N \end{cases}$$

Figure 2.2 shows the number of infected people over time for an example trajectory in the model with $N = 10000$,$\beta = 1.3$,$\gamma = 1$,$\delta = 1$,with initial condition $S(0) = 9000$,$I(0) = 1000$,$R(0) = 0$.

2.1.2 The dynamics of the SIRS model

To find the equilibrium points of this epidemic model, we need to solve for the conditions where the derivatives of each equation are zero. Specifically, we solve the following system of equations:

$$\begin{cases} \frac{dS}{dt} = -\frac{\beta SI}{N} + \delta R = 0 \\ \frac{dI}{dt} = \frac{\beta SI}{N} - \gamma I = 0 \\ \frac{dR}{dt} = \gamma I - \delta R = 0 \end{cases}$$

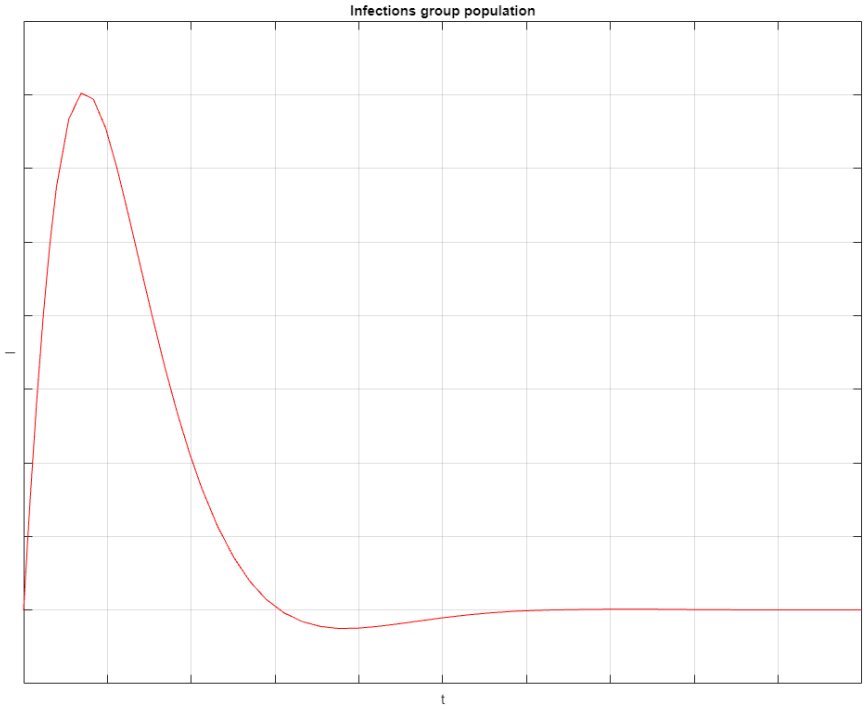

Figure 2.2: SIR flow diagram. The x-axis is time (weeks) while the y-axis represents the number of infections. $N = 10000$,$\beta = 1.3$,$\gamma = 1$,$\delta = 1$,with initial condition $S(0) = 9000$,$I(0) = 1000$,$R(0) = 0$

Starting with the third equation:

$$\gamma I - \delta R = 0 \implies R = \frac{\gamma}{\delta} I$$

Substitute $R = \frac{\gamma}{\delta} I$ into the first equation:

$$-\frac{\beta S I}{N} + \delta \left(\frac{\gamma}{\delta} I\right) = 0 \implies -\frac{\beta S I}{N} + \gamma I = 0 \implies I(\gamma - \frac{\beta S}{N}) = 0$$

This implies $I = 0$ or $\gamma N = \beta S$.

If $I = 0$:

$$\frac{dR}{dt} = \gamma I - \delta R = 0 \implies R = 0$$

and using the initial condition $S + I + R = N$, we get:

$$S = N$$

Therefore, one equilibrium point is:

$$(S, I, R) = (N, 0, 0)$$

If $\gamma N = \beta S$:

$$S = \frac{\gamma N}{\beta}$$

Substituting into $S + I + R = N$ and $R = \frac{\gamma}{\delta} I$ we get:

$$\frac{\gamma N}{\beta} + I + \frac{\gamma}{\delta} I = N \implies \frac{\gamma N}{\beta} + I\left(1 + \frac{\gamma}{\delta}\right) = N$$

$$I = N(\frac{1 - \frac{\gamma}{\beta}}{1 + \frac{\gamma}{\delta}})$$

Substituting I back into $R = \frac{\gamma}{\delta} I$:

$$R = \frac{N\gamma}{\delta}\left(\frac{1 - \frac{\gamma}{\beta}}{1 + \frac{\gamma}{\delta}}\right)$$

Therefore, another equilibrium point is:

$$(S, I, R) = \left(\frac{\gamma N}{\beta}, \frac{(1 - \frac{\gamma}{\beta})N}{1 + \frac{\gamma}{\delta}}, \frac{\gamma N}{\delta}\left(\frac{1 - \frac{\gamma}{\beta}}{1 + \frac{\gamma}{\delta}}\right)\right)$$

The first equilibrium has no infected people ($I = 0$), which is called a "Disease Free Equilibrium (DFE)".

The second equilibrium point represents the equilibrium state of the system under non-zero infection. In the long term, the infection will not disappear completely, but will remain at a stable level. This is consistent with some real-life infectious diseases, such as influenza, which will not be completely eradicated but will persist at a certain level.

The second term of the second equilibrium point suggests that only when

$$1 > \frac{\gamma}{\beta}$$

will the equilibrium point be realistic, since we want the state of the system to remain non-negative because it is the number of people in different classes. It is also worth noting that if $N = \frac{\gamma}{\beta}$, the two equilibrium points are equal. Which

shows the same idea of the basic reproduction umber theory which will be talked about in the next chapter.
Figure 2.3 shows the dynamics of the SIRS system for different initial conditions, $N = 10000$,$\beta = 1.3$,$\gamma = 1$,$\delta = 1$.

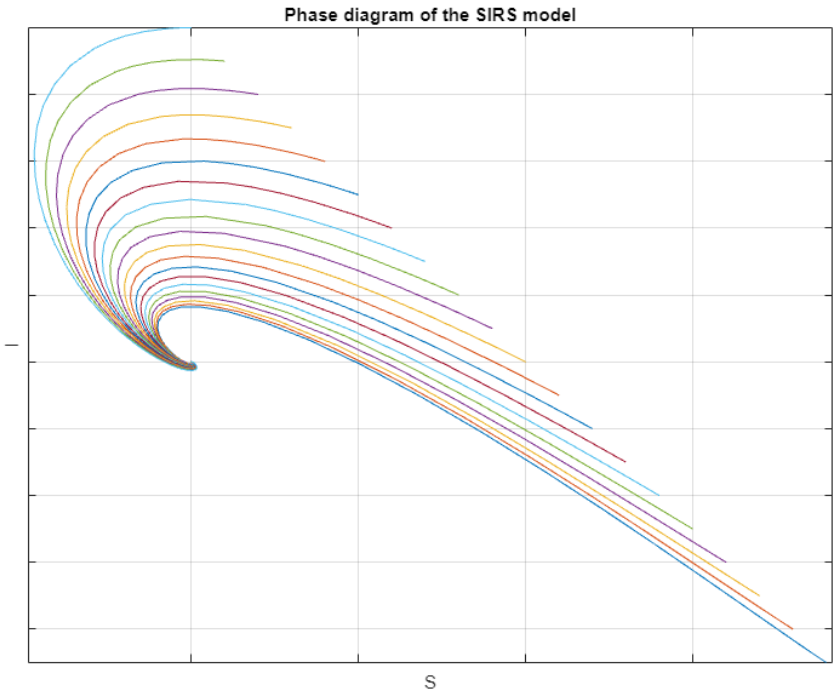

Figure 2.3: SIRS phrase diagram. The x-axis is the number of people in compartment "S" while the y-axis is the number of people in compartment "I"

2.2 Definition of a generalized epidemic system

In order to find a more general method to calculate epidemic thresholds, we need a general and rigorous mathematical definition of the epidemic model. I will discuss this process in detail in Chapter 3, but here we do some preliminary work to ensure the consistency of the model proposed later.

The number of people in all compartments are time based functions. We describe the state of the system at time t by a vector function $X \in C^1(\mathbb{R}_{(t)})$

$$\mathbf{X}_{(t)} = (x_1(t), x_2(t), ..., x_n(t))^T, \forall t \geq 0$$

which means there are n such compartments in the whole system. We say a compartment is infection-related if individuals in that compartment are infected by the disease. If we have just three compartments (S, I and R) as listed above, the only infection-related compartment is the Infected (I) compartment. We now rearrange these compartments as the following way: Let the first m elements of the vector be infection-related and the rest of the vector be non-infection-related.

$$\mathbf{X}(t) = (x_1(t), x_2(t), ..., x_m(t), x_{m+1}(t), ..., x_n(t))^T$$

To describe the out flow and in flow of each compartment we define:

Definition 2:

- $F_i : \mathbb{R}^n \to \mathbb{R}$**:** Rate of new infections flow into compartment "i" .
- $V_i^+(X) : \mathbb{R}^n \to \mathbb{R}$**:** Rate of all flows into compartment "i".
- $V_i^-(X) : \mathbb{R}^n \to \mathbb{R}$**:** Rate of population all flows out from compartment "i".

The disease transmission model is given by:

$$\frac{dx_i}{dt} = F_i(x_{(t)}) - V_i(x_{(t)}), \forall t \geq 0 \forall i = 1, ..., n$$

where $V_i = V_i^- - V_i^+$ for $i = 1, ..., n$.

2.2.1 Model with more compartments – An SEIRS model

Model design

Diseases such as COVID-19 or flu have an incubation period. When an individual is infected by these viruses they won't become contagious immediately. The time from infection until the individual becomes infectious is called the incubation period. We model this by introducing a new compartment "Exposed" to describe this behavior. Also we include the births and deaths into this model.
To set up the system, we need to first define the following parameters in Table 2.1:

Table 2.1: **Parameters in SEIRS model**

Parameter	Description	Range
μ	birth/death rate	$[0, 1]$
β	effective contact rate	$[0, 1]$
N	population	$\mathbb{Z}^+$
ϵ	$\frac{1}{\text{duration of immunity}}$	$\mathbb{Q}^+$
α	$\frac{1}{\text{incubation period}}$	$\mathbb{Q}^+$
δ	$\frac{1}{\text{infectious period}}$	$\mathbb{Q}^+$

During the transmission process, $\frac{\beta I(t)}{N}$ represents the rate that susceptible individuals become infected. This idea is simply because the higher the proportion of infected people, the greater the infection rate.

Now the ODE system is shown as below:

$$\mathbf{X}'(t) = (E(t), I(t), S(t), R(t))^T$$

$$F(X') = \begin{bmatrix} \frac{\beta S(t) I(t)}{N} \\ \alpha E(t) \\ 0 \\ 0 \end{bmatrix}$$

$$V^+(X') = \begin{bmatrix} 0 \\ 0 \\ \mu N + \epsilon R(t) \\ \delta I(t) \end{bmatrix}$$

$$V^{-}(X') = \begin{bmatrix} \alpha E(t) + \mu E(t) \\ \mu I(t) \\ \mu S(t) + \frac{\beta S(t) I(t)}{N} \\ \mu R(t) + \epsilon R(t) \end{bmatrix}$$

$$\frac{d\mathbf{X}'}{dt} = F(X') + V^{+}(X') - V^{-}(X')$$

To make it more readable the system is actually:

$$\begin{cases} \frac{dS}{dt} = -\frac{\beta S_{(t)} I_{(t)}}{N} - \mu S_{(t)} + \epsilon R_{(t)} + \mu N \\ \frac{dE}{dt} = \frac{\beta S_{(t)} I_{(t)}}{N} - \alpha E_{(t)} - \mu E_{(t)} \\ \frac{dI}{dt} = \alpha E_{(t)} - \mu I_{(t)} \\ \frac{dR}{dt} = \delta I_{(t)} - \epsilon R_{(t)} - \mu R_{(t)} \\ S(0) = s_0, \quad s_0 \in \mathbb{R} \\ E(0) = e_0, \quad i_0 \in \mathbb{R} \\ I(0) = i_0, \quad i_0 \in \mathbb{R} \\ R(0) = 0 \\ s_0 + i_0 + e_0 = N \end{cases}$$

Figure 2.4 shows the transmission process of the SEIRS model.

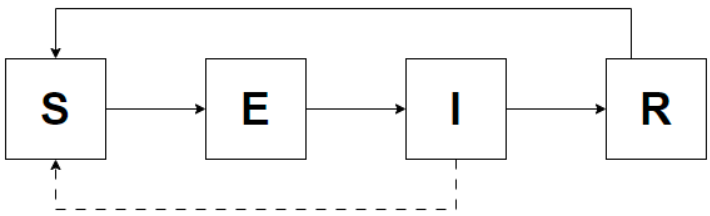

Figure 2.4: SEIRS process diagram, where solid lines indicate flows and dotted lines indicate infection paths)

2.3 Existence and uniqueness of the solution to the SEIRS model

Since time is a continuous variable ranging from 0 to infinity, we need to prove that the ordinary differential equation system has a unique solution on this interval.

Consider the ODE system in this form:

$$\frac{d\mathbf{y}_{(\mathbf{t})}}{dt} = \mathbf{g}(t; \mathbf{y}_{(t)}),$$

with the initial condition:

$$\mathbf{y}(t_0) = \mathbf{y_0} \in \mathbf{R^n}$$

for some function

$$g : \mathbb{R}_+ \times \mathbb{R}^n \to \mathbb{R}$$

We say that $\mathbf{g}$ satisfies the local Lipschitz condition on a domain $G \subset \mathbb{R}_+ \times \mathbb{R}^n$ if, for any point $(t_0, \mathbf{y_0})$ in G, there is a closed neighborhood $R \subset G$, and a constant $L > 0$, so that the inequality:

$$||\mathbf{g}(t; \widetilde{\mathbf{y}}) - \mathbf{g}(t; \overline{\mathbf{y}})|| \leq L||\widetilde{\mathbf{y}} - \overline{\mathbf{y}}||$$

holds for all $(t, \widetilde{\mathbf{y}}) \in \mathbb{R}$. We call L the (Local) Lipschitz's constant of G.

Theorem 1: Let $(t_0, y_0) \in \mathbb{R}_+ \times \mathbb{R}^n$ If a vector function $\mathbf{g}$ is continuous and satisfies the local Lipschitz condition on a domain containing a closed neighborhood $R = \{(t, y) \in \mathbb{R}_+ \times \mathbb{R}^n; |t - t_0| \leq a \quad ||y - y_0|| \leq b\}$ of (t_0, y_0) then the equation

$$\begin{cases} \frac{dy_{(t)}}{dt} = g(t, y_{(t)}) \quad \forall t \in [t_0 - a, t_0 + a] \\ y(t_0) = y_0 \end{cases}$$

has a unique solution $\mathbf{y} = \phi(\mathbf{t}; t_0, \mathbf{y_0})$ which is continuous on domain $[t_0 - h, t_0 + h]$ where $h = min(a, \frac{b}{M})$, $M = max\{||\mathbf{g}(t, \mathbf{y})||, (\mathbf{t}, y) \in \mathbf{R}\}$

To prove the existence and the uniqueness of the solution to the SEIRS system, the idea is to show that $F + V$ is Lipschitz.

Proof. Rewrite $F + V$ as:

$$\mathbf{g}(t; S, E, I, R) = \begin{bmatrix} -\mu S - \frac{\beta SI}{N} + \mu N + \epsilon R \\ \frac{\beta SI}{N} - \alpha E - \mu E \\ -\mu I + \alpha E - \delta I \\ -\mu R - \epsilon R + \delta I \end{bmatrix}$$

By calculating the Jacobian of $g(t, 0) : \mathbb{R}^4 \to \mathbb{R}^4$, we get:

$$J(S, E, I, R) = \begin{bmatrix} -\mu - \frac{\beta I(t)}{N} & 0 & -\frac{\beta S(t)}{N} & \epsilon \\ \frac{\beta I(t)}{N} & -\alpha - \mu & \frac{\beta S(t)}{N} & 0 \\ 0 & \alpha & -\mu & 0 \\ 0 & 0 & \delta & -\mu - \epsilon \end{bmatrix}$$

Since the norm of $J(S, E, I, R) = (a_{ij})_{1 \leq i,j \leq 4}$ is (up to a constant) bounded $max|a_{ij}|, 1 \leq i, j \leq 4$ and since μ, N, α, ϵ are all constant, we only need a bound on the terms by contain S or I. As these terms are linear in S, I, they are locally bounded.

This means that g is locally Lipschitz (with respect to $\mathbf{y}$) on $\mathbb{R}$. From the mid value theorem, we can conclude that the system has a unique solution for $|\mathbf{t}| \leq h$ with $h = min(a, \frac{b}{M})$, $M = max\{||\mathbf{g}(t, \mathbf{y})||, (\mathbf{t}, y) \in \mathbf{R}\}$, and $\mathbf{R} = [0, h] \times B(y(0), N)$

□

2.4 The seasonality of diseases

One thing that cannot be ignored in epidemiology is that many diseases are seasonal. Seasonality means that some infectious diseases will have a higher number of patients at some times of the year and correspondingly, a lower number of patients will appear at other times. This pattern occurs regularly each year. A good example is influenza. Therefore, adding seasonality to our model would allow it to better capture epidemics with seasonal characteristics. We introduce seasonality by adjusting the transmission parameter β to include a sinusoidal forcing function:

$$\beta(t) = \beta_0(\beta_1 sin(\frac{2\pi}{356}t) + 1) \quad \forall t \geq 0$$

Note that β_0 represents the average transmission rate while β_1 represents the

strength of the seasonality.

2.4.1 The existence of solution

Since β is no longer a constant, we need to consider the existence of solutions in the new system. We can see that although β now changes with time, it still has an upper bound and a lower bound which are 0 and β_0. So that will not change the identity of the previous proof. In other words, the solution still exists, and it is unique on $t \in (O, +\infty))$

2.4.2 Simulation of the seasonality model

Here we show the effect of the strength of seasonality.

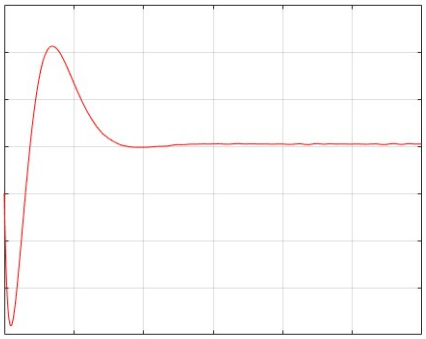

Figure 2.5: $\beta_1 = 0$

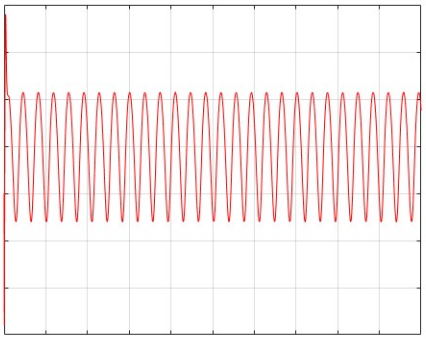

Figure 2.6: $\beta_1 = 0.2$

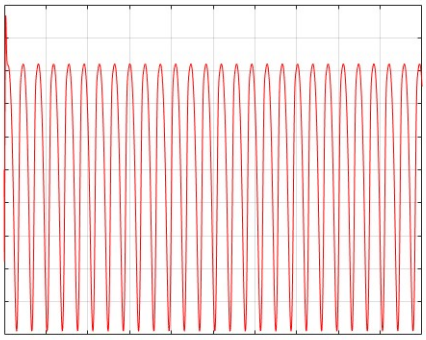

Figure 2.7: $\beta_1 = 0.5$

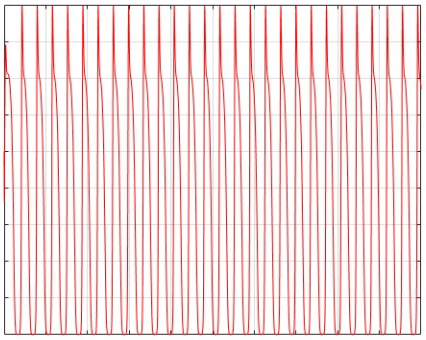

Figure 2.8: $\beta_1 = 1$

Figure 2.9: All the x-axis and y-axis of the sub-figures represent the time (weeks) and the number of infections, respectively.

Chapter 3

Basic reproduction number R_0

3.1 Epidemiological interpretation

In epidemiological studies, it is often believed that there are certain thresholds that determine whether there will be an outbreak of an infectious diseases. The population threshold mentioned in the analysis of the SIRS model above is one of them. In this chapter we will discuss a new commonly used threshold, the "Basic reproduction number", which we often refer to as R_0.

The epidemiological definition of R_0 is:

The expected number of secondary cases produced by a typical infected individual during its entire infectious period, in a population consisting of susceptibles only[6].

This threshold represents the number of new cases created by each infected person throughout the disease cycle. We believe that when R_0 is greater than 1, an epidemic of the disease will occur, and when R_0 is less than 1, the disease will die out in the population. In fact, the value of R_0 is also linked to the stability of the system of differential equations. When R_0 is less than 1, the system will be stable near the Disease Free Equilibrium, otherwise it's unstable.

P. van den Driessche [18] proposed an efficient way to calculate R_0 in his paper. It's called the "Next Generation Matrix Method". In this chapter we will discuss the mathematical definition of the next generation matrix and reproduce the relevant proofs for the stability of the ODE system.

3.2 Expansion of model assumptions

Recall the model we set up in **Definition 1** and **Definition 2**. The model is given in the form of:

$$\frac{dx_i}{dt} = f_i(x) = F_i(x) - V_i(x)$$

where $V_i(x) = V_i^-(x) - V_i^+(x)$ and $i \in \mathbb{Z}^+$, while the first m compartments in the system are infection-related and the rest of the terms are not infection-related. We expect the system to satisfy the following 5 assumptions.

Definition 3: We call a set in the form of

$$X_s = \{x \geq 0 | x_i = 0, i = 1, ..., m\}$$

the set of all **Disease Free States**.

We make some bioloically relevant assumptions on $F_i, V_i^+, V_i^-, i = 1, ..., n$.

- **A1:** If $x \geq 0$, then $F_i(x), V_i^+(x), V_i^-(x) \geq 0$ for $i \in [1, n], i \in \mathbb{Z}$
  This is because these three parts all represent the rate flowing into or out of a certain compartment, so they cannot be negative.

- **A2:** if $x_i = 0$ then $V_i^-(x) = 0$. In particular, if $x \in X_s$ then $V_i^-(x) = 0$ for $i = 1, ..., m$.
  This is because if the compartment is empty then there can't exist any flow out from it.

- **A3:** $F_i, V_i^+ = 0$ if $i > m$
  This condition affirms that the uninfected compartments are always uninfected.

- **A4:** if $x \in X_s$ then $F_i(x) = 0$ and $V_i^+(x) = 0$ for $i = 1, ..., m$
  The idea of this assumption is that the **DFE** is an invariant which means that once the population is free of disease, there system will stay disease free. In particular, the infection-related groups will no longer have any new infections.

- **A5:** If F_i is set to zero, consider the linearized system around the **DFE**:

$$\dot{x} = Df(x_0)(x - x_0)$$

. Here, $Df(x_0)$ is the Jacobian matrix of the system evaluated at the **DFE**. Then all eigenvalues of $Df(x_0)$ have negative real parts.

The explanation of **A5** needs a further theorem:
Consider the following **ODE** system:

$$\frac{d\mathbf{x}}{dt} = f(\mathbf{x}(t)), \mathbf{x}(0) = \mathbf{x}_0$$

where $\mathbf{x}(t) \in U \subset \mathbb{R}^n$ and $f : U \to \mathbb{R}^n$, where f has equilibrium at $\mathbf{x}^*$ such that $f(\mathbf{x}^* = 0)$. Consider the linearization of the system we get:

$$\frac{d\mathbf{x}}{dt} = \mathbf{A}\mathbf{x}(t)$$

where A is the Jacobian of the system. We introduce the following Theorem.
Theorem 2: The equilibrium x^* of an ODE system:

$$\frac{d\mathbf{x}}{dt} = \mathbf{A}f(\mathbf{x}(t)), \mathbf{x}(0) = \mathbf{x}_0$$

is asymptotically stable if and only if all eigenvalues of the operator A have negative real parts.

Under the background of epidemiology we want to restrict our attention to systems in which the DFE is stable in the absence of new infections. From theorem 2 we can see that if x_0 is an DFE and $Df(x_0)$ is negative, then we can conclude that the system is asymptotically stable. This means that if there is a small number of infected individuals introduced to the system, it will return to the DFE according to the linearized system:

$$\frac{d\mathbf{x}}{dt} = Df(x_0)(x - x_0)$$

3.3 Partition of the operator $Df(x_0)$

Definition 4 (Z-matrix): A matrix of the form $A = sI - B$ with $B \geq 0, s \geq 0$ is said to have the Z-sign pattern. Equivalently, a matrix has the Z-sign pattern

if every off-diagonal entry is negative or 0.

Definition 5 (M-matrix):. An M-matrix is a Z-matrix where $s \geq \rho(B)$. Equivalently, an M-matrix is a Z-matrix with eigenvalues whose real parts are positive.

Lemma 1: If x_0 is a DFE of the system we defined before and $f_i(x)$ satisfy **A1-A5**, then $DF(x_0)$ and $DV(x_0)$ could be written as:

$$DF(x_0) = \begin{pmatrix} F & 0 \\ 0 & 0 \end{pmatrix}, DV(x_0) = \begin{pmatrix} V & 0 \\ J_3 & J_4 \end{pmatrix}$$

where F and V are the $m \times m$ matrices defined by

$$F = [\frac{\partial F_i}{\partial x_j}(x_0)]$$

and

$$V = [\frac{\partial V_i}{\partial x_j}(x_0)]$$

with $1 \leq, j \leq m$. Further, F is non-negative, V is a non-singular M-matrix and all eigenvalues of J_4 have positive real part.

Proof. **(1) partition and zero blocks:**
By (A3) and (A4) we can see that if $x_0 \in X_s$ is a DFE, then we have $\frac{\partial F_i}{\partial x_j}(x_0) = 0$ if $i > m$ or $j > m$. This is because the compartments later than m are all uninfected compartments. Similar, by (A2) and (A4) we can conclude that if $x_0 \in X_s$ then $V_i(x) = 0$ for $i \leq m$. Thus,$\frac{\partial V_i}{\partial x_j}(x_0) = 0$ for $i \leq m$ and $j > m$. This shows the partition and zero blocks.(A1) and (A4) als shows the Non-negativity of F obviously.

(2) V is a non-singular M-matrix:
Let e_j be the Euclidean basis vectors. That is, e_j is the j^{th} column of the $n * n$ identity matrix. Then, for $j = 1, ..., m$,

$$\frac{\partial V_i}{\partial x_j}(x_0) = \lim_{h \to 0^+} (\frac{V_i(x_0 + he_j) - V_i(x_0)}{h})$$

Since $x_0 \in X_s$, by (A2) and (A4), $V_i(x_0) = 0$ for $i = 1, ..., m$, and if $i \neq j$, then the i^{th} component of $x_0 + he_j = 0$ and $V_i(x_0 + he_j) \leq 0$, by (A1) and (A2). Hence,

$\frac{\partial(V_i)}{\partial(x_j)} \leq 0$ for $i \leq m$ and $j \neq i$ and V has the Z sign pattern. Additionally, by (A5), all eigenvalues of V have positive real parts. These two conditions imply that V is a non-singular M-matrix. Condition (A5) also implies that the eigenvalues of J_4 have positive real part.

□

3.4 Calculate the R_0 with NGM

Considered the linearized system:

$$\frac{d\mathbf{x}}{dt} = Df(x_0)(x - x_0)$$

when the re-infection is turned off (i.e $F_i = 0, \forall i = 1, ..., n$)it becomes (substituting the partitioned matrix):

$$\frac{d\mathbf{x}}{dt} = -DV(x_0)(x - x_0)$$

By (A5), the system at the DFE is asymptotically stable, so the linearized system could be used to describe the behavior of a small number of infected individuals introduced to a disease free population.

Let $\phi_i(0)$ be the number of infected individuals introduced into infected compartment i at time 0, and let $\phi(t) = (\phi_1(t), ..., \phi_m(t))$ be the number of individuals in the infected compartments at time t.

$\frac{d\mathbf{x}}{dt} = -DV(x_0)(x - x_0)$ is actually in the following format:

$$\begin{pmatrix} \frac{d\phi(t)}{dt} \\ \cdots \end{pmatrix} = - \begin{pmatrix} V & 0 \\ J_3 & J_4 \end{pmatrix} \begin{pmatrix} \phi(t) \\ \cdots \end{pmatrix} = \begin{pmatrix} -V\phi(t) \\ \cdots \end{pmatrix}$$

which implies that:

$$\frac{d\phi(t)}{dt} = -V\phi(t)$$

which has the known solution

$$\phi(t) = e^{-Vt}\phi(0)$$

According to Lemma 1, the matrix V is a non-singular M-matrix, so it is invertible, and all of its eigenvalues have positive real parts. Therefore, integrat-

ing the function $F\phi(t)$ from zero to infinity gives the expected number of new infections caused by the initially infected individuals, represented as the vector $FV^{-1}\phi(t)$. Since F is non-negative and V is a non-singular M-matrix, V^{-1} is non-negative, and thus FV^{-1} is also non-negative.

The (i, k) entry of the product FV^{-1} shows the expected number of new infections in compartment i produced by the infected individual originally introduced into compartment k. Thus, we define FV^{-1} to be the "Next Generation Matrix" and define the basic reproduction number:

$$R_0 = \rho(FV^{-1})$$

where $\rho(A)$ denotes the spectral radius of a matrix A.

3.5 Stability and R_0

Lemma 2. *Let H be a non-singular M-matrix and suppose B and BH^{-1} have the Z sign pattern. Then B is a non-singular M-matrix if and only if BH^{-1} is a non-singular M-matrix.*

Lemma 3. *Let H be a non-singular M-matrix and suppose $K \geq 0$. Then,*

(i) $(H - K)$ is a non-singular M-matrix if and only if $(H - K)H^{-1}$ is a non-singular M-matrix.

(ii) $(H - K)$ is a singular M-matrix if and only if $(H - K)H^{-1}$ is a singular M-matrix.

The proof of lemma 2 and 3 could be found in [18]

Theorem 3: Consider the ODE model given above with $f(x)$ satisfied all 5 assumptions. If x_0 is a DFE of the system, then it is asymptotically stable if $R_0 < 1$ and unstable when $R_0 > 1$

Proof. Let $J_1 = F - V$, where: F is a non-negative matrix representing the transmission part of the disease. V is a non-singular M-matrix representing other transition processes.

Since V is a non-singular M-matrix, it has positive diagonal elements, non-positive off-diagonal elements, and $V^{-1} \geq 0$. Because $F \geq 0$, we can write:

$$J_1 = F - V = -(V - F).$$

Thus, J_1 has the Z sign pattern , meaning its off-diagonal elements are non-positive and diagonal elements are non-negative. Let $s(J_1)$ denote the maximum real part of all eigenvalues of J_1. For matrices with the Z sign pattern, J_1 is a non-singular M-matrix if and only if $s(J_1) < 0$:

$$s(J_1) < 0 \quad \iff \quad J_1 \text{ is a non-singular } M\text{-matrix.}$$

Since $V^{-1} \geq 0$ and $F \geq 0$, it follows that $FV^{-1} \geq 0$. Consider the matrix:

$$-J_1V^{-1} = -(F - V)V^{-1} = -FV^{-1} + VV^{-1} = I - FV^{-1}.$$

This matrix also has the Z sign pattern. By Lemma 2, with $H = V$ and $B = -J_1 = V - F$, we have:

$-J_1$ is a non-singular M-matrix $\iff$ $I - FV^{-1}$ is a non-singular M-matrix.

Since $FV^{-1} \geq 0$, all eigenvalues of FV^{-1} are non-negative. The largest eigenvalue of FV^{-1} is its spectral radius $\rho(FV^{-1})$. Therefore:

$$I - FV^{-1} \text{ is a non-singular } M\text{-matrix} \quad \iff \quad \rho(FV^{-1}) < 1.$$

Define $R_0 = \rho(FV^{-1})$. Combining the above results:

$$s(J_1) < 0 \quad \iff \quad R_0 < 1.$$

Applying Lemma 3, with $H = V$ and $K = F$, we obtain:

$s(J_1) = 0$ $\iff$ $-J_1$ is a singular M-matrix $\iff$ $I - FV^{-1}$ is a singular M-matrix

Thus:

$$s(J_1) = 0 \quad \iff \quad R_0 = 1.$$

From the above, we conclude:

$$\begin{cases} s(J_1) < 0 & \text{if and only if } R_0 < 1, \\ s(J_1) = 0 & \text{if and only if } R_0 = 1, \\ s(J_1) > 0 & \text{if and only if } R_0 > 1. \end{cases}$$

□

3.6 An example of calculating R_0 with NGM:

We now calculate the R_0 of the SEIRS model. Recall that

$$\mathbf{X}'(t) = (E(t), I(t), S(t), R(t))^T$$

$$\mathcal{F}(X') = \begin{bmatrix} \frac{\beta S(t) I(t)}{N} \\ 0 \\ 0 \\ 0 \end{bmatrix}$$

$$\mathcal{V}(X') = \begin{bmatrix} \alpha E(t) + \mu E(t) \\ \mu I(t) - \alpha E(t) + \delta I(t) \\ \mu S(t) + \frac{\beta S(t) I(t)}{N} - \mu N - \epsilon R(t) \\ \mu R(t) + \epsilon R(t) - \delta I(t) \end{bmatrix}$$

Thus calculating the Jacobian at the DFE and by Lemma 1 we obtain:

$$F = \begin{bmatrix} 0 & \beta \\ 0 & 0 \end{bmatrix}$$

and

$$V = \begin{bmatrix} \alpha + \mu & 0 \\ -\alpha & \delta + \mu \end{bmatrix}$$

then we get:

$$V^{-1} = \begin{bmatrix} \frac{1}{\alpha+\mu} & 0 \\ \frac{\alpha}{(\alpha+\mu)(\delta+\mu)} & \frac{1}{\mu} \end{bmatrix}$$

Thus the NGM is:

$$FV^{-1} = \begin{bmatrix} \frac{\alpha\beta}{(\alpha+\mu)(\delta+\mu)} & 0 \\ 0 & 0 \end{bmatrix}$$

By calculating the eigenvalues of this matrix, we get:

$$R_0 = \rho(FV^{-1}) = \frac{\alpha\beta}{(\mu+\alpha)(\delta+\mu)}$$

Chapter 4

Vaccines

4.1 Basic assumptions

As vaccines are a commonly used method to control seasonal diseases such as influenza, we add vaccination to the model to obtain simulation results that are more in line with reality using the following assumptions:

- *A*6**:** The vaccines are not 100% effective.
- *A*7**:** Only people that are not currently infected by the disease are willing to be vaccinated, which means only people in group S or R will be vaccinated. Here we ignore the vaccination of people in group E since the incubation period of Covid-19 and flu is relatively shorter [11][17] than the length of the period that vaccination is available[1][14].
- *A*8**:** The vaccines will only be available in a certain time period and the effect will only last for a certain length of time[1][14].

4.2 Design of the vaccine function

According to (A7), vaccines will only be available at a fixed time period during the year, which means the function needs the ability to describe this feature. Ideally, the square wave function (Figure 4.1) is a appropriate choice since it is periodic and has a shape that fits the assumption.

However, the introduction of the square wave function may affect the Lipschitz continuity of the SEIRS system that we proved in Chapter 2, that is, it may cause the solution of the entire system to not exist or be non-unique. Therefore,

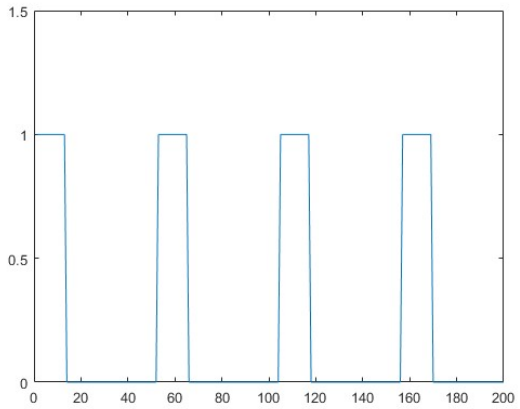

Figure 4.1: Square wave function

we smooth the square wave function to a certain extent to ensure its continuity. We will use the variable m to describe the week of the year in which vaccination was initiated, while q is a constant that sets the slope of the mediating function that bridges the gap between full and no vaccine availability. In addition, the vaccine function we define should be a periodic function with a period of 52. Therefore, we define the function $\phi(t)$ as:

- $m = 0$ **to** 35**:**

$$\phi_{\text{periodic}}(x) = \begin{cases} 0, & 0 \leq x \mod 52 < m, \\ q \cdot (x \mod 52 - m), & m \leq x \mod 52 < m + 1, \\ q, & m + 1 \leq x \mod 52 < m + 16, \\ -q \cdot (x \mod 52 - m - 16) + 17q, & m + 16 \leq x \mod 52 < m + 17, \\ 0, & m + 17 \leq x \mod 52 < 52. \end{cases}$$

- $m = 36$ **to** 52**:**

$$\phi_{\text{periodic}}(x) = \begin{cases} q, & 0 \leq x \mod 52 < m - 36, \\ -q \cdot (x \mod 52 - (m - 35)), & m - 36 \leq x \mod 52 < m - 35, \\ 0, & m - 35 \leq x \mod 52 < m - 1, \\ q \cdot (x \mod 52 - m) + q, & m - 1 \leq x \mod 52 < m, \\ q, & m \leq x \mod 52 < 52. \end{cases}$$

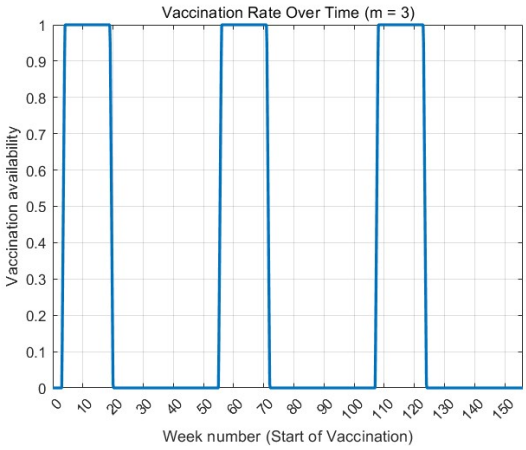

Figure 4.2: vaccine function $\phi(t)$ with $m = 3$

We also need to normalize ϕ, so divide ϕ by a normalization constant $16q$, which is 1600 here. Due to the simplicity of the form, the derivation process is omitted here. From A6, we know that the vaccine is not 100% effective and the coverage of the vaccine is limited. Therefore, we introduce the variables $\tau \in [0, 1]$ and $k \in [0, 1]$ to describe the probability of the vaccine successfully protecting the vaccine recipient and the coverage of the vaccine, respectively. Since the S and R groups are the only sources of vaccine recipients, and the vaccine coverage is calculated based on the entire population, the total number of vaccine recipients $N * coverage$ should be distributed equally according to the number of people in the S and R groups. Therefore, the expression for the number of vaccine recipients $V_s(t)$ from the S group and the number of vaccine recipients $V_r(t)$ from the R group are:

$$V_S(t) = \frac{N * coverage}{S(t) + R(t)} * \frac{\phi(t)}{16q} * S(t)$$

$$V_R(t) = \frac{N * coverage}{S(t) + R(t)} * \frac{\phi(t)}{16q} * R(t)$$

Figure 4.2 shows the $\phi(t)$ function with the vaccine available at the third week of each year.

4.3 New compartments for the SEIRS model

After the introduction of the vaccine, we will add a new compartment V to our model to describe the people who have gained immunity through the vaccine. In

addition, the effectiveness is not perfect (some people are not protected), and the duration of protection is not permanent. After the expiration date, the people in compartment V will return to compartment S. We define a constant $\theta \in [0, 1]$ as the inverse of the vaccine effective duration. Thus the flows in and flow out of compartment V can be discribed as:

$$V(t) = V_S(t) + V_R(t) - \theta * V(t)$$

Now, we state the ODE system:

$$\begin{cases} \frac{dS}{dt} = -\beta_0 \left(\beta_1 \sin\left(\frac{2\pi(t-\kappa)}{52}\right) + 1\right) \frac{SI}{N} - \frac{Nk\tau\phi(t)}{16q(S+R)} S + \theta V + \epsilon R + \mu N - \mu S, \\ \frac{dE}{dt} = \beta_0 \left(\beta_1 \sin\left(\frac{2\pi(t-\kappa)}{52}\right) + 1\right) \frac{SI}{N} - \alpha E - \mu E, \\ \frac{dI}{dt} = \alpha E - \delta I - \mu I, \\ \frac{dR}{dt} = \delta I - \epsilon R - \frac{Nk\tau\phi(t)}{16q(S+R)} R - \mu R, \\ \frac{dV}{dt} = \frac{Nk\tau\phi(t)}{16q(S+R)} R + \frac{Nk\tau\phi(t)}{16q(S+R)} S - \theta V - \mu V \\ s_0 + e_0 + i_0 + r_0 + v_0 = N \end{cases}$$

The flow chart for the SEIRS model with vaccine is shown in figure 4.3.

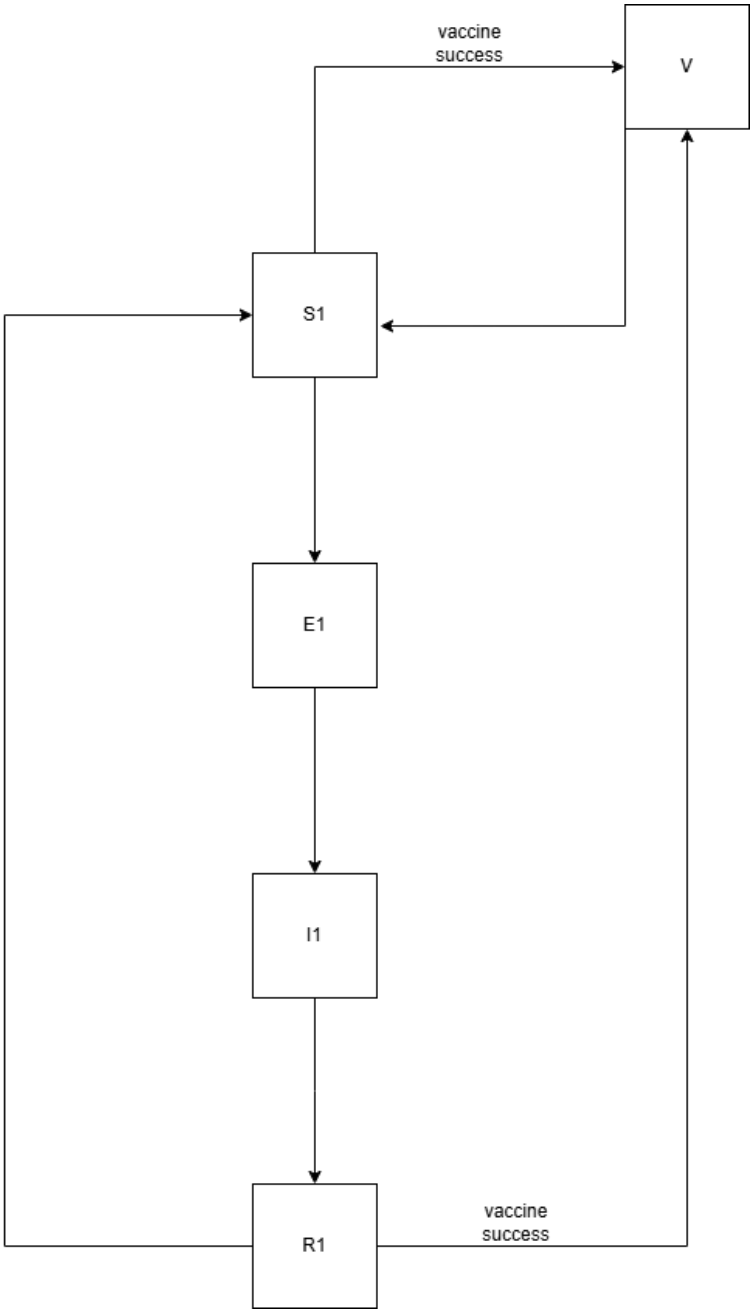

Figure 4.3: SEIRS model with vaccine

4.4 Numerical Solutions to the model with vaccine

Based on the data on influenza in Table 4.1, we numerically solved the model. In this model, the total population N is set to the total Australian population of

26955026, and birth and death rates are considered constant. In addition, the average transmission rate is calculated directly from the basic reproduction number formula derived above. Since the numerical simulation results in this chapter are mainly used to present seasonal patterns and the impact of vaccine coverage, the effectiveness of the vaccine is considered to be 100%, and the seasonal intensity is set to 0.16, which is chosen as an example. In actual analysis, it should be optimally fitted. We will discuss the parameters that need to be optimized in the model and the corresponding regularization principles in the next chapter. From the model numerical simulation results (Figure 4.4), we can see that as vaccine coverage increases, the number of infected people drops significantly, which is in line with our expectations and common sense. Among them, the difference of vaccine coverage from 0% to 20% is the most significant, which confirms the rationality of the model establishment. In other words, the vaccine equation we added does indeed play a role in blocking the spread of influenza. In addition, as vaccine coverage increases, the number of infections continues to approach 0. It can be observed that the vaccine coverage threshold for complete elimination of influenza from the population should be between 0.6 and 0.8. The intervention of the vaccine changes the effective reproduction number, forcing it to be lower than the original basic reproduction number, thus achieving control of the disease. It is important to note here that the current model assumes that vaccine effectiveness is uniform across age groups. In actual epidemic control, we have to consider the differences in the effects of vaccines on different age groups. For example, it is mentioned in [14] that there are significant differences in the effects of influenza vaccines on different age groups. In addition, vaccine coverage and population mortality rates actually vary among different age groups. To describe the above issues more accurately, we need to consider establishing a SEIRVS model with age structure, which we will discuss in Chapter 5. In addition, in this chapter we assume that the effective contact rate of the population is not the same across all age groups.

Table 4.1: Parameter Descriptions and Values of influenza

Parameter	**Description**	**Value**	**Source**
μ	Birth and death rate	0.0121	[2]
ϵ	Immunity period	$\frac{1}{26}$	[19]
β_0	Average transmission rate	1.3	Calculation based on [17]
β_1	Seasonality strength	0.16	By assumption
N	Population	$26,955,026$	[10]
α	Incubation period	$\frac{7}{1.4}$	[17]
δ	Infection period	1	[17]
k	Vaccine coverage rate	0.274	Government data
τ	Vaccine effectiveness	0.59	[14]
m	Time of vaccine (week)	$(0, 52]$	By assumptions
v	Vaccine effective duration	$1/26$	[12]

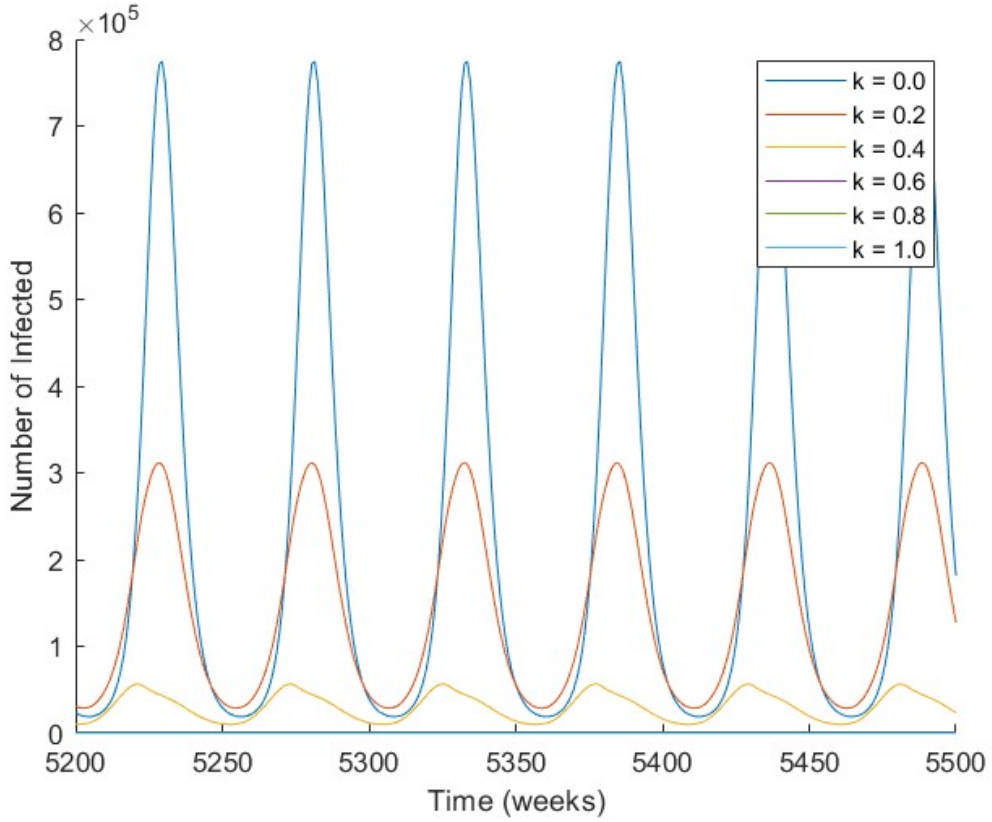

Figure 4.4: Number of influenza cases under different vaccine coverage levels (k).

Chapter 5

Parameter estimation

In the numerical simulation of the influenza model in Chapter 3, we assumed that the seasonal shifting factor κ was 0, and also made assumptions about the seasonal intensity. Since the influenza data set is relatively complete and has shown a good stable trend, we can estimate the values of these parameters based on data, so that the numerical solution of the model is closer to the actual situation. In this chapter, I will explain the statistical principle of L-1 and L-2 regularization and fit an SEIRS influenza model based on a system of ordinary differential equations as an example to demonstrate the process of L-1 and L-2 regularization and analyze which regularization method is more effective for the SEIRS model of influenza. In addition, the parameter estimation results obtained by the algorithm will be used to conduct numerical simulations of the ODE system and serve as secondary evidence of the regularization effect. The regularization methods discussed in this chapter will also be used in the parameter estimation process in Chapters 5 and 6.

5.1 Selection of regularization methods

We perform parameter estimation using a portion of the Australian National Notifiable Disease Surveillance System (NNDSS) influenza dataset. Since the NNDSS data set is based on laboratory-confirmed cases, it does not capture all infected people. Not all influenza-infected people will go to hospitals or professional testing institutions to confirm the type of virus they are infected with. Therefore, we assume that 1 out of every 10 influenza infected people will go to the corresponding medical institution for testing. Based on this assumption, we amplified the original data by 10 times during the parameter estimation process.

Since the principle of regularization is based on the prior estimation of parameters based on data, we observed the data characteristics presented in Figure 5.1 and found that they show good symmetry and central trend. This means that the rate of change in the number of infected people on both sides of the peak is symmetrical and distributed around a certain mean. Therefore we can assume that our target parameters exhibit a Gaussian or Laplace distribution. This is the reason we choose L1 and L2 regularization, and their equivalence will be discussed in subsequent chapters.

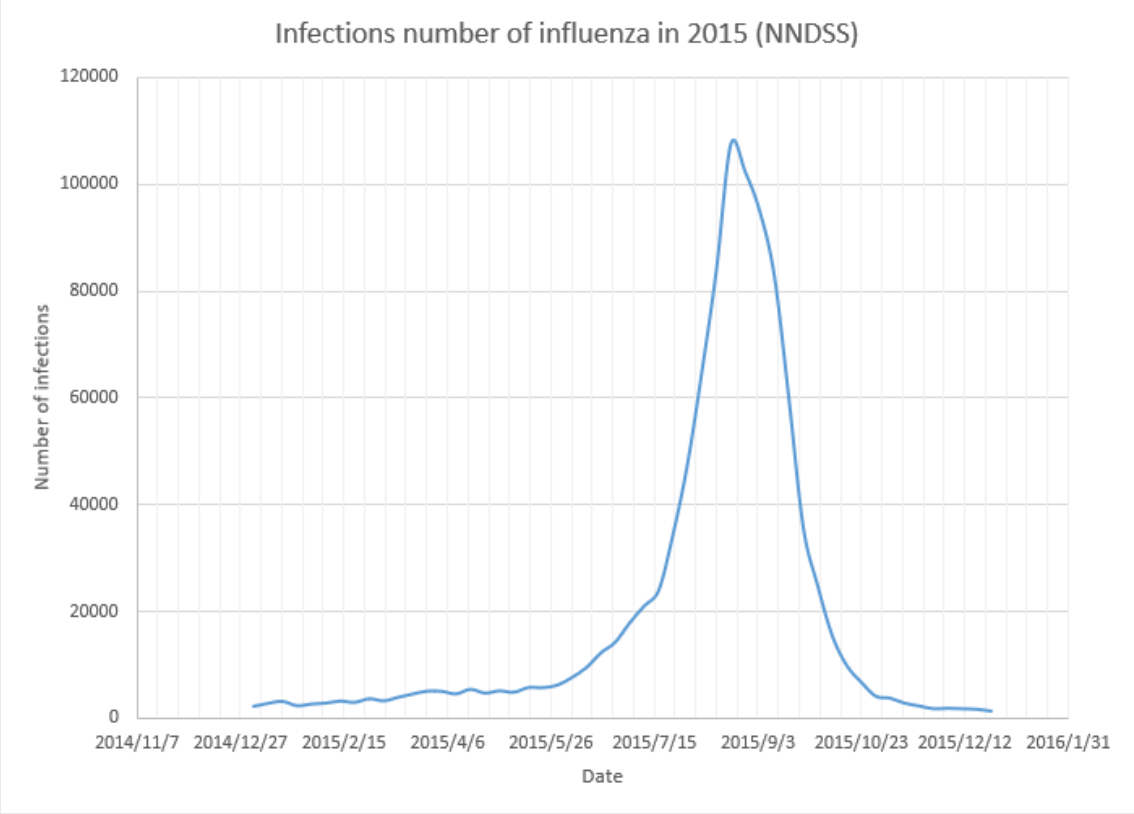

Figure 5.1: Number of influenza infections in 2015 from NNDSS

5.2 L-1 and L-2 regularization:

The purpose of regularization is to decrease over-fitting by limiting model complexity. We often achieve regularization by adding an extra real value function $\Omega(\rho)$ of the objective parameters $\rho \in \mathbb{R}^5$ to the objective function to impose a so-called "penalty" on high-complexity models. Suppose the original cost func-

tion is: $J(\rho; X, y)$ where ρ are the parameters and X, y are the corresponding variables and data. In this paper, X is $[S_1, I_1, E_1, R_1, V]$.

Then we can give the general term of the regularization problem:

$$\tilde{J}(\rho; X, y) = J(\rho; X, y) + \xi\Omega(\rho)$$

The constant ξ is the strength of the regularization while the function Ω is called the regularization term by computational mathematicians. In this study $J(\rho; X, y)$ is actually the sum of squares residual:

$$J(\rho; X, y) = \sum_{i=1}^{n}(y_i - X_i\rho)^2$$

Definition 3: L-1 Regularization could be achieved through setting the regularization term as the L-1 norm of the parameters, which is:

$$\Omega(\rho) = ||\rho||_1 = \sum_{i=1}^{n}|\rho_i|$$

Definition 4: L-2 Regularization could be achieved through setting the regularization term as the L-2 norm squared of the parameters, which is:

$$\Omega(\rho) = ||\rho||_2^2 = \sum_{i=1}^{n}\rho_i^2$$

By adding regularization terms, we redefine the optimization problem:
For L1 regularization: $\min_\rho \left(\sum_{i=1}^{n}(y_i - X_i\rho)^2 + \xi\sum_i|\rho_i|\right)$
For L2 regularization: $\min_\rho \left(\sum_{i=1}^{n}(y_i - X_i\rho)^2 + \xi\sum_i\rho_i^2\right)$

5.3 The Bayesian explanation of regularization:

Recall Bayes' theorem:

$$P(\rho|Data) = \frac{P(Data|\rho)P(\rho)}{P(Data)}$$

In this part, I will show the equivalence between adding an L-1 regularization term and the assumption that parameters follow a Laplace prior distribution with $mean = 0$. Meanwhile, I also show the equivalence between adding an L-2 regularization term and the assumption that parameters follows a Gaussian prior distribution with $mean = 0$.

Consider a regression model in the following format:

$$y = X\rho + \Phi$$

where y is the observation data vector, X is the compartments variable (i.e. S_1,E_1,I_1,R_1,V), ρ is the weight vector and Φ is the random error. We assume $\Phi \sim N(0, \sigma^2 I)$ where I is an identity matrix. Since y is a linear transformation of Φ, we can say that y follows a normal distribution when X and ρ are both given, which is:

$$y|X, \rho \sim N(X\rho, \sigma^2 I)$$

and the likelihood function $P(y|X, \rho)$ could be given as:

$$P(y|X, \rho) \propto exp(-\frac{1}{2\sigma^2}||y - X\rho||_2^2)$$

Now we assume that ρ follows a Gaussian prior distribution with $mean = 0$ ($\rho \sim N(0, \tau^2 I)$) and we can conclude that:

$$P(\rho) \propto exp(-\frac{1}{2\tau^2}||\rho||_2^2)$$

From the Bayesian theorem, we can rewrite the Posterior probability $P(\rho|y)$ as the product of the prior probability and the likelihood function:

$$P(\rho|y) \propto P(y|\rho)P(\rho) \propto exp(-\frac{1}{2\sigma^2}||y - X\rho||_2^2 - \frac{1}{2\tau^2}||\rho||_2^2)$$

We take the Log of the Posterior probability:

$$L(\rho) = -\frac{1}{2\sigma^2}||y - X\rho||_2^2 - \frac{1}{2\tau^2}||\rho||_2^2$$

$$= -(\frac{1}{2\sigma^2}||y - X\rho||_2^2 + \frac{1}{2\tau^2}||\rho||_2^2)$$

then computing the maximum of $L(\rho)$ is equivalent to finding the minimum of the cost function:

$$\tilde{J}(\rho; X, y) = \frac{1}{2\sigma^2}||y - X\rho||_2^2 + \frac{1}{2\tau^2}||\rho||_2^2$$

We can see that the first term of $\tilde{J}(\rho; X, y)$ is exactly the sum of squares of the residuals, and the second term is the L-2 regularization term.

For L-1 regularization, if we assume the Laplace distribution ($mean = 0$ and the parameter is a) as the prior distribution of ρ, we can get similar result that it is equivalent to adding a L-1 regularization term to the loss function.

5.4 Effect analysis of L-1 and L-2:

In this section, I'm going to explain the property that: L-1 and L-2 regularization both reduce algorithm complexity by limiting the parameter space. This explanation is given from the perspective of geometry and KKT theory.

Theorem 3: Karush-Kuhn-Tucker Theorem:
Suppose we have a minimization problem in the following form:

$$\begin{aligned} &\text{minimize } J(\rho) \\ &\text{subject to } \begin{cases} c_i(\rho) = 0 & \text{for } i = 1, \cdots, m_e, \\ c_i(\rho) \leq 0 & \text{for } i = m_e + 1, \cdots, m, \end{cases} \end{aligned}$$

where J and c_i are smooth real-valued functions on $\mathbb{R}^n$, and m_e and m are non-negative integers with $m_e \leq m$. We set

$$\mathcal{E} := \{1, \cdots, m_e\} \quad \text{and} \quad \mathcal{I} := \{m_e + 1, \cdots, m\}.$$

Let $\rho^* \in \mathcal{F}$ be a local minimizer of this problem. LFD(x) is the Linearized

Feasible Directions at point x, $T_{\rho^*}\mathcal{F}$ is the tangent cone of of F at x. If

$$T_{\rho^*}\mathcal{F} = \text{LFD}(\rho^*),$$

then there exists $\lambda^* = (\lambda_1^*, \ldots, \lambda_m^*)^T \in \mathbb{R}^m$ such that

$$\nabla J(\rho^*) + \sum_{i \in \mathcal{E} \cup \mathcal{I}} \lambda_i^* \nabla c_i(\rho^*) = 0,$$

$$c_i(\rho^*) = 0 \quad \text{for all } i \in \mathcal{E},$$
$$c_i(\rho^*) \leq 0 \quad \text{for all } i \in \mathcal{I},$$
$$\lambda_i^* \geq 0 \quad \text{for all } i \in \mathcal{I},$$
$$\lambda_i^* c_i(\rho^*) = 0 \quad \text{for all } i \in \mathcal{E} \cup \mathcal{I}.$$

Adding a regularization term to the objective function is equivalent to adding an inequality constraint to the feasible set. Here, we take L1 regularization as an example to show that it is equivalent to adding an inequality constraint on the L1 norm of the parameters in an optimization problem. For L2, the principle will be very similar. To be more specific, let t be a constant, then consider the L-1 regularization of the problem $\min_\rho J(\rho; X, y)$ which is:

$$\min_\rho \left(\sum_i (y_i - X_i\rho)^2 + \xi \sum_i |\rho_i| \right)$$

We are going to show that it is equivalent to:

$$\min_\rho J(\rho; X, y)$$

$$s.t. ||\rho||_1 \leq t$$

In other words, we want to show that the following two optimization problems are equivalent under certain conditions.

$$\min_{\rho \in \mathbb{R}^n} \quad J(\rho) + \lambda \|\rho\|_1$$

where $J(\rho)$ is a convex, differentiable objective function, $\lambda > 0$ is the regularization strength, and $\|\rho\|_1 = \sum_{i=1}^n |\rho_i|$ is the L1 norm of the parameter vector ρ.

$$\begin{aligned} \min_{\rho \in \mathbb{R}^n} \quad & J(\rho) \\ \text{subject to} \quad & \|\rho\|_1 \leq t \end{aligned}$$

where $t > 0$ is a constant that constrains the L1 norm of the parameters. We aim to show that there exists a correspondence between these two problems: for a given $\lambda > 0$, there exists a $t > 0$ such that the solutions to both problems coincide, and vice versa.

For the constrained problem:

$$\begin{aligned} \min_{\rho} \quad & J(\rho) \\ \text{s.t.} \quad & \|\rho\|_1 \leq t \end{aligned}$$

we can construct the Lagrangian:

$$L(\rho, \lambda) = J(\rho) + \lambda(\|\rho\|_1 - t)$$

where $\lambda \geq 0$ is the Lagrange multiplier. From Theorem 3 we get the Karush-Kuhn-Tucker (KKT) conditions for a solution ρ^* to be optimal including:

$$\|\rho^*\|_1 \leq t$$

$$\lambda^* \geq 0$$

$$\lambda^*(\|\rho^*\|_1 - t) = 0$$

$$\nabla J(\rho^*) + \lambda^* \nabla \|\rho^*\|_1 = 0$$

The condition $\lambda^*(\|\rho^*\|_1 - t) = 0$ implies:

If $\lambda^* > 0$, then $\|\rho^*\|_1 = t$ and if $\lambda^* = 0$, then $\|\rho^*\|_1 < t$.

If the constraint is active ($\lambda^* > 0$, $\|\rho^*\|_1 = t$), then the stationarity condition becomes:

$$\nabla J(\rho^*) + \lambda^* \nabla \|\rho^*\|_1 = 0$$

This is equivalent to solving the following unconstrained optimization problem:

$$\min_{\rho} \quad J(\rho) + \lambda^* \|\rho\|_1$$

where $\lambda^* > 0$ is the regularization parameter.

Thus, for any given $t > 0$, if the constraint is active ($\|\rho^*\|_1 = t$), there exists $\lambda^* > 0$ such that the solution to the unconstrained problem with L1 regularization coincides with the solution to the constrained problem. Similarly, for any given $\lambda > 0$, there exists a corresponding t such that the two problems have the same solution. If the constraint is not active ($\lambda^* = 0$) then the two problems are exactly the same.

5.4.1 Geometric interpretation of L-1:

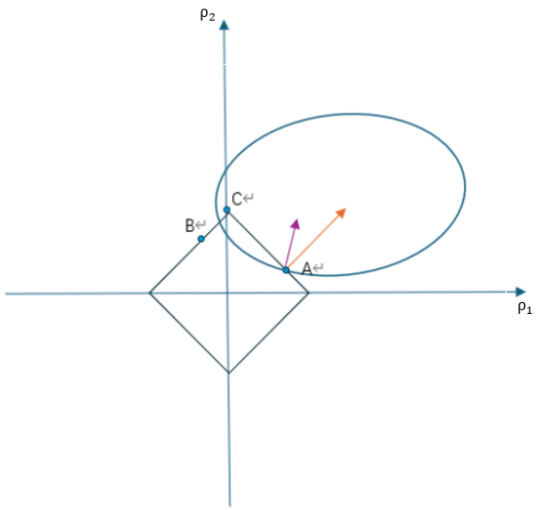

Figure 5.2: L1 regularization for 2 dimensions. The x and y axes represent the values of parameters ρ_1 and ρ_2, respectively. The purple arrow indicates the normal vector of the ellipse at point A, while the orange arrow indicates the normal vector of the square at point A.

Consider a two-dimensional scenario. In this coordinate system, the x and y axes represent the values of two target parameters. In Figure 5.2, the horizontal and vertical coordinates are the values of the two parameters. The corresponding inequality constraint is:

$$|\rho_1| + |\rho_2| \leq M$$

The interior and boundary of the square represent the parameter space, corresponding to the inequality constraints mentioned earlier. Since we use the sum of squared residuals as the objective function, the contours of the objective function are elliptical. Suppose our initial value is at point C. We know that the normal vector of the ellipse at point C and the direction vector of the square at point C point towards the direction of change at point C. Clearly, since point C cannot reach outside the square, it can only move along the side of the square towards the Y-axis until it reaches the Y-axis. When the two normal vectors overlap, the movement stops. We get an optimal solution with one parameter being zero and the other taking a constant value. Similarly, in higher dimensions, the norm ball changes from a square to a cube, and the ellipse changes to an ellipsoid. Guided by the normal vectors, the optimization result stops when most parameters reach zero at point C, demonstrating sparsity. In this way, we expect to get a parameter matrix which is sparse. In other words, we can expect more parameters are 0 when we use L-1 regularization, which means the optimization process selects the parameters that contribute most to the model.

5.4.2 Geometric interpretation of L-2:

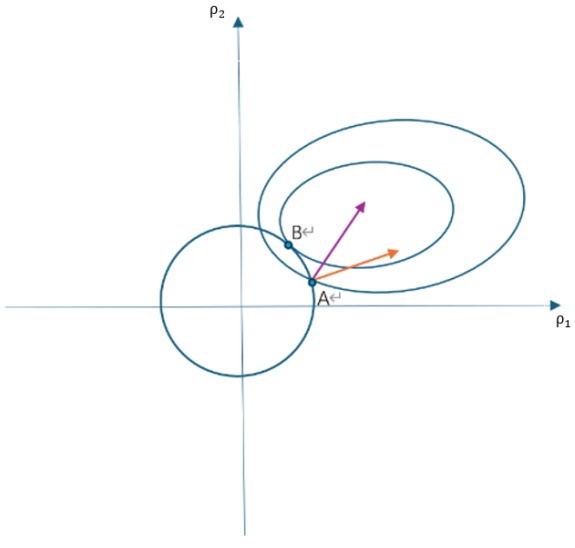

Figure 5.3: L-2 regularization for 2 dimensions. The x and y axes represent the values of parameters ρ_1 and ρ_2, respectively. The purple arrow indicates the normal vector of the ellipse at point A, while the orange arrow indicates the normal vector of the square at point A.

Similarly, Figure 5.3 shows the feature of L-2 regularization (two-dimensional). Point A will move in the direction of the sum of the normal vectors until they overlap. That is, the optimal solution is obtained at point B.

5.5 Application to influenza data

We are going to use the NNDSS data to verify the effect of L-1 and L-2 regularization. Since influenza is a seasonal disease, we adjust β from a constant to a function of t:

$$\beta(t) = \beta_0(\beta_1 sin(\frac{2\pi}{52}(t-\kappa)+1))$$

β_0 is the average transmission rate, β_1 is the strength of seasonality and κ is the phase of seasonality.

The goal parameters are β_1 and κ. We combine L1 and L2 regularization together so we have our regularization terms as follows:

$$||w||_1 + ||w||_2^2 = \lambda_1(|\kappa| + |\beta_1|) + \lambda_2(\kappa^2 + \beta_1^2)$$

where the constants λ_1 and λ_2 represent the regularization strength.

We define the initial values for the parameters according to Table 5.1.

Table 5.1: Parameter Descriptions and Values for influenza

Parameter	**Description**	**Value**	**Source**
μ	Birth and death rate	0.0121	[2]
ϵ	Immunity period	$\frac{1}{26}$	[19]
β_0	Average transmission rate	1.3	Calculation based on [17]
β_1	Seasonality strength	$[0, inf]$	
κ	Seasonality shifting factor	$[0, 52]$	
N	Population	$26,955,026$	[10]
α	Incubation period	$\frac{7}{1.4}$	[17]
δ	Infection period	1	[17]
λ_1	regularization strength for L1	10000000	
λ_2	regularization strength for L2	10000000	

The Pseudo code is given as below:

Algorithm 1 Parameter Optimization and Simulation

Load data:
Read the data set into variable `d`
Set global variable `true_i`
`true_i = d(:, 1)(1:52)` ▷ Use the first 52 rows from the first column
Set the lower and upper bounds for parameters:
`lb = [0, 0]` ▷ Lower bounds for [`beta_1`, `season_shift`]
`ub = [10, 52]` ▷ Upper bounds for [`beta_1`, `season_shift`]
Set initial parameter values:
`x0 = [0.2, 0]` ▷ Initial values for [`beta_1`, `season_shift`]
Perform parameter optimization using `fmincon`:
Call `fmincon` to optimize the objective function `seir_Obj_fun`
Pass initial values `x0` and bounds `lb`, `ub`
Obtain optimized values `x` and the objective function value `fval`
Extract optimized parameters:
`beta_1 = x(1)`
`season_shift = x(2)`
Set simulation time `T`:
`T = length(true_i)` ▷ T = 52
Define fixed parameters: beta_0, alpha, delta, mu, epsilon, N
Simulate the model using the optimized parameters:
Call `ode45` with the function `seir_fun` to compute the simulation results
Set time range as `[1:T]`
Initial conditions are `[N-1, 0, 1, 0]`
Store the simulation results in `p`
Plot the results:
Plot simulation results `p(:, 3)` and real data `true_i`
Add legend, labels, and title
Define the SEIR model's ODE equations:
Function `seir_fun` takes inputs `t`, `x`, and model parameters
Compute the SEIR model derivatives `dp`
Define the objective function `seir_Obj_fun` for optimization:
Function `seir_Obj_fun` takes optimization parameters `x`
Extract parameters `beta_1` and `season_shift`
Simulate the model using the optimization parameters
Compute the objective function value `f`
The objective function is the sum of squared differences between the simulation and real data, plus a regularization term

5.5.1 Result and interpretation:

The specific values we get are $\beta_1 = 0.1619$ and $\kappa = 6.6154$. Figure 5.4 shows the simulation result compared with the NNDSS data set, which demonstrates that the results of the numerical simulation are consistent with the trends in the data. The peak number of infected people occurs in week 40, which means that July to October each year is the peak period of influenza in Australia, which is consistent with actual experience.

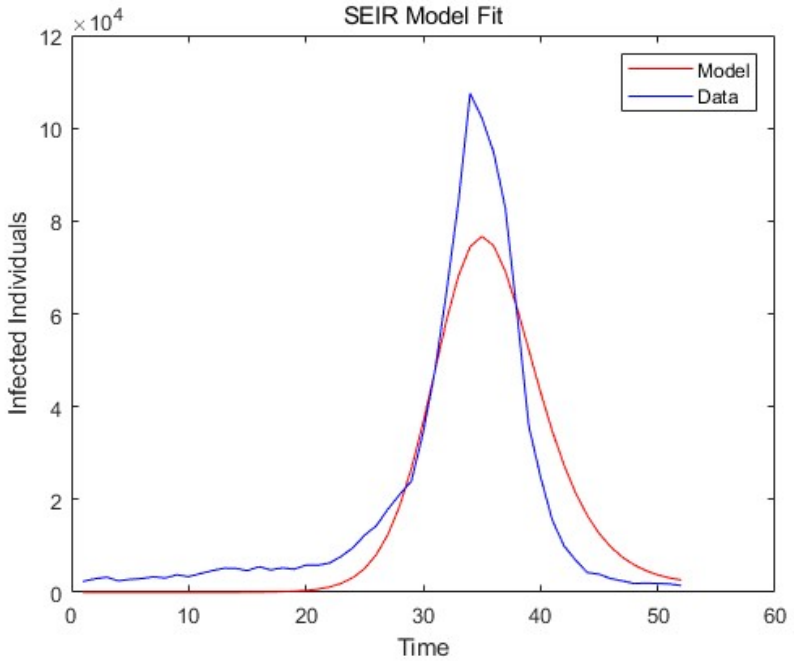

Figure 5.4: Simulation result of the Flu-SEIR model

Chapter 6

Age structure model

In the previous chapter, we discussed the establishment and data simulation of the SEIRS model. This is based on the assumption that the population is uniformly distributed. In other words, the probability of people of any age group coming into contact with each other and spreading the epidemic is equally likely. In addition, the coverage and effectiveness of the vaccine are also assumed to be the same across all ages. Such a model setting can roughly describe the spread of seasonal diseases in the population, but it is missing key features. Through the research of Sullivan and others[14] and the research of Xia [19] and others, it can be seen that the immune effects of vaccines in people of different age groups are very significant. In addition, research by Mistry and others [9] shows that people of different age groups do not have equal exposure opportunities, so the effective contact rate of the disease is different. This is due to their social preferences, living habits, frequent places and social relationships.

In existing research, there are two ways to express the age structure. The first is to introduce a new age variable to turn the entire SIR system into a continuous partial differential system. This method has not been widely adopted because of the high computational complexity of its numerical solution. Although the PDE model can improve the accuracy of the model, according to actual experience, it does not make a significant difference in describing the trend of the epidemic. In fact, establishing an ODE dynamic system by discretizing the age structure (that is, treating the population of a certain age group as a new "compartment") can accurately describe the epidemic trend of diseases and greatly reduces the computational complexity. In addition, in epidemiological surveys, data collection is often carried out according to different age groups, rather than for every differ-

ent year of age. Therefore, from a data perspective, choosing to build an ODE model by age group is more consistent with the data structure than building a continuous PDE model.

6.1 Age structure model set up

As described in the previous section, we need to adjust the compartments of the model and some variable settings. Based on the previous SEIRS model, we extend it as follows. Introduce compartments S_i, E_i, I_i, R_i to describe the S, E, I, R classes for age group i. In addition, define an $n \times n$ matrix β, in which the element β_{ij} is used to describe the effective contact rate of individuals in age group i relative to individuals in age group j. In this research, we set each age class as the same length. Denote the time of an individual spent in one age class as ω_i. A compartment with age i will receive new members from the corresponding compartment with age i-1, and then flow out to the corresponding compartment with age i+1. (That is, compartment S_i will receive the population flowing out of S_{i-1}, and then flow into S_{i+1}).

Using these new setups, we can derive an SEIRS model with age-structure for a seasonal disease as below:

for $i = 1, 2, 3..., n$ and $j = 1, 2, 3..., n$

$$\frac{dS_1}{dt} = -\sum_{j=1}^{n}\left(\beta_1 \sin\left(\frac{2\pi(t-\kappa)}{52}\right)+1\right)\frac{\beta_{1j}S_1 I_j}{N} + \epsilon R_1 - \frac{1}{\omega}S_1 + \mu N$$

$$\frac{dE_1}{dt} = \sum_{j=1}^{n}\left(\beta_1 \sin\left(\frac{2\pi(t-\kappa)}{52}\right)+1\right)\frac{\beta_{1j}S_1 I_j}{N} - \alpha E_1 - \frac{1}{\omega}E_1$$

$$\frac{dI_1}{dt} = \alpha E_1 - \delta I_1 - \frac{1}{\omega}I_1$$

$$\frac{dR_1}{dt} = \delta I_1 - \epsilon R_1 - \frac{1}{\omega}R_1$$

$$\vdots$$

$$\frac{dS_i}{dt} = -\sum_{j=1}^{n}\left(\beta_1 \sin\left(\frac{2\pi(t-\kappa)}{52}\right)+1\right)\frac{\beta_{ij}S_iI_j}{N} + \epsilon R_i - \frac{1}{\omega}S_i + \frac{1}{\omega}S_{i-1}$$

$$\frac{dE_i}{dt} = -\sum_{j=1}^{n}\left(\beta_1 \sin\left(\frac{2\pi(t-\kappa)}{52}\right)+1\right)\frac{\beta_{ij}S_iI_j}{N} - \alpha E_i - \frac{1}{\omega}E_i + \frac{1}{\omega}E_{i-1}$$

$$\frac{dI_i}{dt} = \alpha E_i - \delta I_i - \frac{1}{\omega}I_i + \frac{1}{\omega}I_{i-1}$$

$$\frac{dR_i}{dt} = \delta I_i - \epsilon R_i - \frac{1}{\omega}R_i + \frac{1}{\omega}R_{i-1}$$

With initial conditions:

$$S_i(0) = S_{i_0}, E_i(0) = E_{i_0}, I_i(0) = I_{i_0}, R_i(0) = R_{i_0}, V_i(0) = V_{i_0}$$

$$S_{i_0} + E_{i_0} + I_{i_0} + R_{i_0} + V_{i_0} = N_{i_0}$$

$$\sum_{i=1}^{n} N_{i_0} = N$$

6.2 Introduction of the vaccine

By adjusting the vaccine function defined in 4.3, we now set the age structure of the compartment V based on the original variables. That is, the population of the compartment V_i with age i comes from the population that successfully obtains immunity through vaccination in S_i and R_i, and the population that enters from V_{i-1} due to age growth, and will also flow out of the population to V_{i+1}. In addition, similar to 3.3, the population whose immunity fails will return to S_i. Death is also considered in this process.

In order to keep the proportion of the population protected by the vaccine constant, we adjust the vaccine function in 4.3. First, define N_i as the total population of age group i:

$$N_i = S_i + E_i + I_i + R_i$$

Secondly, the function ϕ is normalized and then proportionally distributed to $V_{S_i}(t)$ and $V_{R_i}(t)$, resulting in the following form:

$$V_{S_i}(t) = \frac{N_i * k_i * \tau_i}{S_i(t) + R_i(t)} * \frac{\phi(t)}{16q} * S_i(t)$$

$$V_{R_i}(t) = \frac{N_i * k_i * \tau_i}{S_i(t) + R_i(t)} * \frac{\phi(t)}{16q} * R_i(t)$$

Finally, the vaccine compartment $V_i(t)$ for age group i is:

$$V_i(t) = V_{S_i}(t) + V_{R_i}(t) - \theta V_i(t) - \frac{1}{\omega} V_i(t) + \frac{1}{\omega} V_{i-1}(t) - \mu V_i$$

Combine the vaccine equation and the age structure model we get the final SEIRVS model:

for $i = 1, 2, 3..., n$

$$\frac{dS_1}{dt} = -\sum_{j=1}^{n}\left(\beta_{1j}\sin\left(\frac{2\pi(t-\kappa)}{52}\right)+1\right)\frac{\beta_0 S_1 I_j}{N} - \frac{N_1 k_1 \tau_1 \phi(t) S_1(t)}{16q(S_1(t)+R_1(t))} + \theta V_1 + \epsilon R_1$$

$$-\frac{1}{\omega}S_1 + \mu N,$$

$$\frac{dE_1}{dt} = \sum_{j=1}^{n}\left(\beta_{1j}\sin\left(\frac{2\pi(t-\kappa)}{52}\right)+1\right)\frac{\beta_0 S_1 I_j}{N} - \alpha E_1 - \frac{1}{\omega}E_1,$$

$$\frac{dI_1}{dt} = \alpha E_1 - \delta I_1 - \frac{1}{\omega}I_1,$$

$$\frac{dR_1}{dt} = \delta I_1 - \epsilon R_1 - \frac{N_1 k_1 \tau_1 \phi(t) R_1(t)}{16q(S_1(t)+R_1(t))} - \frac{1}{\omega}R_1,$$

$$\frac{dV_1}{dt} = V_{S_1}(t) + V_{R_1}(t) - \theta V_1(t) - \frac{1}{\omega}V_1(t),$$

$$\vdots$$

$$\frac{dS_i}{dt} = -\sum_{j=1}^{n}\left(\beta_{ij}\sin\left(\frac{2\pi(t-\kappa)}{52}\right)+1\right)\frac{\beta_0 S_i I_j}{N} - \frac{N_i k_i \tau_i \phi(t) S_i(t)}{16q(S_i(t)+R_i(t))} + \theta V_i + \epsilon R_i$$

$$-\frac{1}{\omega}S_i + \frac{1}{\omega}S_{i-1},$$

$$\frac{dE_i}{dt} = -\sum_{j=1}^{n}\left(\beta_{ij}\sin\left(\frac{2\pi(t-\kappa)}{52}\right)+1\right)\frac{\beta_0 S_i I_j}{N} - \alpha E_i - \frac{1}{\omega}E_i + \frac{1}{\omega}E_{i-1},$$

$$\frac{dI_i}{dt} = \alpha E_i - \delta I_i - \frac{1}{\omega} I_i + \frac{1}{\omega} I_{i-1},$$

$$\frac{dR_i}{dt} = \delta I_i - \epsilon R_i - \frac{N_i k_i \tau_i \phi(t) R_i(t)}{16q(S_i(t) + R_i(t))} - \frac{1}{\omega} R_i + \frac{1}{\omega} R_{i-1},$$

$$\frac{dV_i}{dt} = V_{S_i}(t) + V_{R_i}(t) - \theta V_i(t) - \frac{1}{\omega} V_i(t) + \frac{1}{\omega} V_{i-1}(t),$$

Figure 6.1 shows the flow chart of a model with 3 age classes as an example.

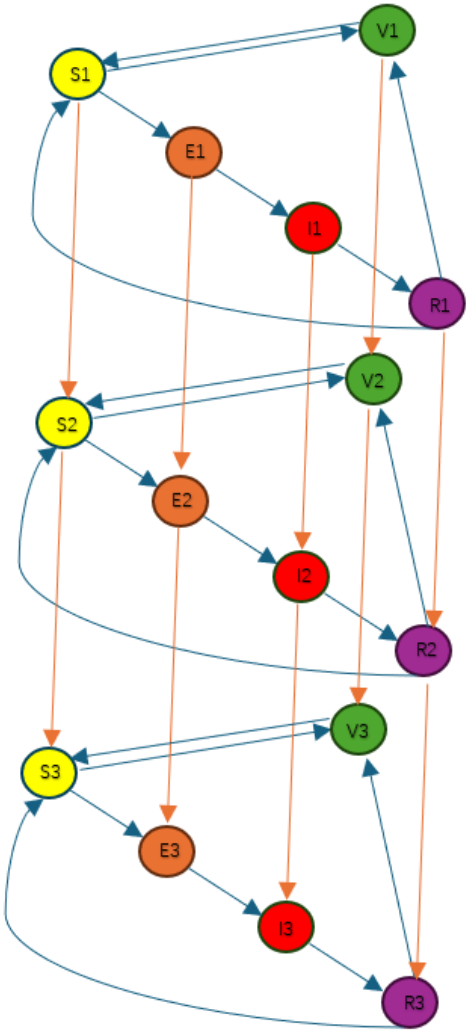

Figure 6.1: Age structure flowchart

Chapter 7

Analysis of the vaccine intervention timing

7.1 Parameter estimation of the Age-structured model

7.1.1 Age structure settings

In order to adapt to the selected data structure, we divide the population into 18 uniform age structures, namely 1-5 6-10 11-15 16-20 21-25 26-30 31-35 36-40 41-45 46-50 51-55 56-60 61-65 66-70 71-75 75-80 80-85 and 85+. Since the time unit of our model is a week, the parameter ω can be estimated as follows:

$$\omega = 52 * 10 = 520$$

This also means that $i = 1, 2, 3, 4, 5, 6, 7, 8, 9$.

7.1.2 The influenza contact matrices

As we defined previously, the effective contact rate between different age groups is different. We use the contact matrix between different age groups provided by Mistry's [9] study to estimate β_{ij}. The contact matrix element M_{ij} can then be thought of as representing the per capita number of contacts an individual of age i has with individuals of age j. In Chapter 3, we calculated the average effective contact rate of influenza using R_0 to be 1.3. We scale the contact matrix to achieve an average contact rate equal to this value. Here we sum all elements

and divide by the number of age groups 18, and get the original contact rate of 11.50591. Therefore, the scaling parameter is $\frac{1.3}{11.50591}$, that is, we multiply each value of the original matrix by this scaling parameter, and finally get the effective contact rate matrix as shown in Figure 7.1

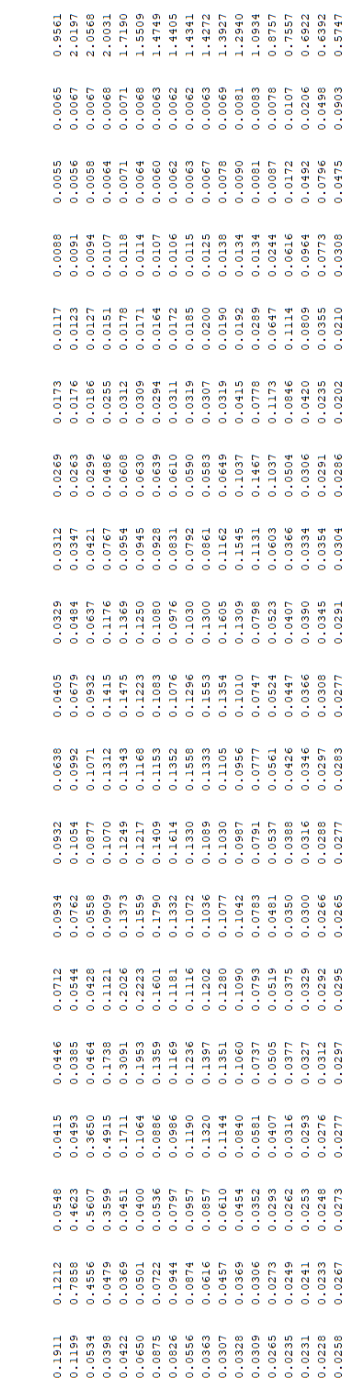

Figure 7.1: Effective contact rate matrix of influenza

Figure 7.2 provided the heatmap of the β matrix of influenza. The horizontal and vertical axes represent different age groups. The brighter the cell, the higher the effective contact rate between the corresponding age groups.

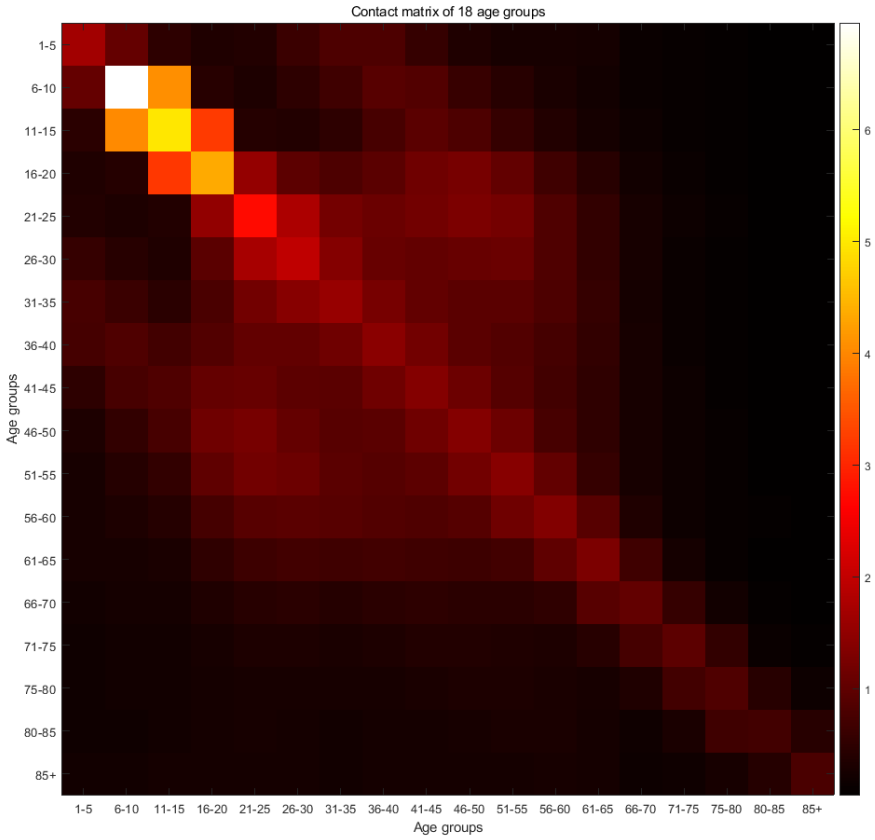

Figure 7.2: Heat map of the effective contact rate matrix. The brighter the area, the higher the effective contact rate.

7.1.3 Influenza vaccine coverage rate

Based on the research of S. G. SULLIVAN [14], we estimate the influenza vaccination coverage as table 7.1 shows:

7.1.4 Influenza vaccine effectiveness

Based on the research of Jennifer M. Radin [12], since we have estimated the duration of protection of the influenza vaccine to be 26 weeks in Chapter 4, we use the average of the vaccine effectiveness in the first 180 days in the original data as the estimate of vaccine effectiveness for the corresponding age group (see the Appendix for the original data). We estimate the influenza vaccination effectiveness as table 7.2 shows:

Age class	Vaccine coverage rate
1-10	6%
11-20	7%
21-30	16%
31-40	16%
41-50	22.5%
51-60	34%
61-70	53.5%
71-80	73%
80+	73%

Table 7.1: Vaccine coverage by age group

Age class	Vaccine effectiveness rate
1-10	66%
11-20	68.5%
21-30	63.25%
31-40	58%
41-50	58%
51-60	58%
61-70	58%
71-80	58%
80+	58%

Table 7.2: Vaccine effectiveness by age group

Table 7.3 shows all parameters of the influenza age-structured model.

Parameter	Description	Value	Source
τ_1	Age 1-10	66%	[12]
τ_2	Age 11-20	68.5%	[12]
τ_3	Age 21-30	63.25%	[12]
τ_4	Age 31-40	58%	[12]
τ_5	Age 41-50	58%	[12]
τ_6	Age 51-60	58%	[12]
τ_7	Age 61-70	58%	[12]
τ_8	Age 71-80	58%	[12]
τ_9	Age 80+	58%	[12]
k_1	Age 1-10	6%	[14]
k_2	Age 11-20	7%	[14]
k_3	Age 21-30	16%	[14]
k_4	Age 31-40	16%	[14]
k_5	Age 41-50	22.5%	[14]
k_6	Age 51-60	34%	[14]
k_7	Age 61-70	53.5%	[14]
k_8	Age 71-80	73%	[14]
k_9	Age 80+	73%	[14]
μ	Birth and death rate (weeks)	$\frac{0.0121}{52}$	[2]
ϵ	Immunity period	$\frac{1}{26}$	[19]
β_{ij}	effective contact rate between age classes	β_{ij}	
β_1	Seasonality strength	0.1619	
N	Population	$26,955,026$	[10]
α	Incubation period	$\frac{7}{1.4}$	[17]
δ	Infection period	1	[17]
k	Vaccine coverage rate	0.274	Government data
τ	Vaccine effectiveness	0.59	[14]
m	Time of vaccine becomes available	$(0, 52]$	By assumptions
θ	Vaccine effective duration	1/26	[12]
κ	seasonality shifting factor	6.6154	[12]

Table 7.3: Parameter Descriptions and Values of influenza

7.1.5 The COVID-19 contact matrices

Similar to influenza, we can derive the scaling factor for COVID-19 as 0.136452 and get the corresponding β matrix as shown in Figure 7.3:

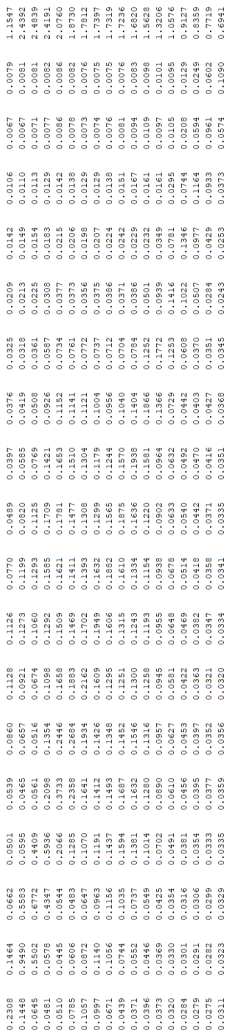

Figure 7.3: Effective contact rate matrix of COVID-19

7.1.6 The COVID-19 Seasonality

By observing the data of COVID-19 in 2022 from covid-19 Australia [3] the (Figure 7.4), we assume that it has a certain seasonality, but its seasonal characteristics are not yet as strong as those of influenza. Therefore, the seasonal intensity is set as $\beta_1 = 0.1$. In addition, regarding the seasonal offset parameter κ, since the peak in the data occurs in the 12th week, we shift the seasonal function to the right by 12 units, that is, set $\kappa = 12$. We have now completed

the estimation of the parameters of the COVID-19 model and all the parameters used are presented in Table 7.4.

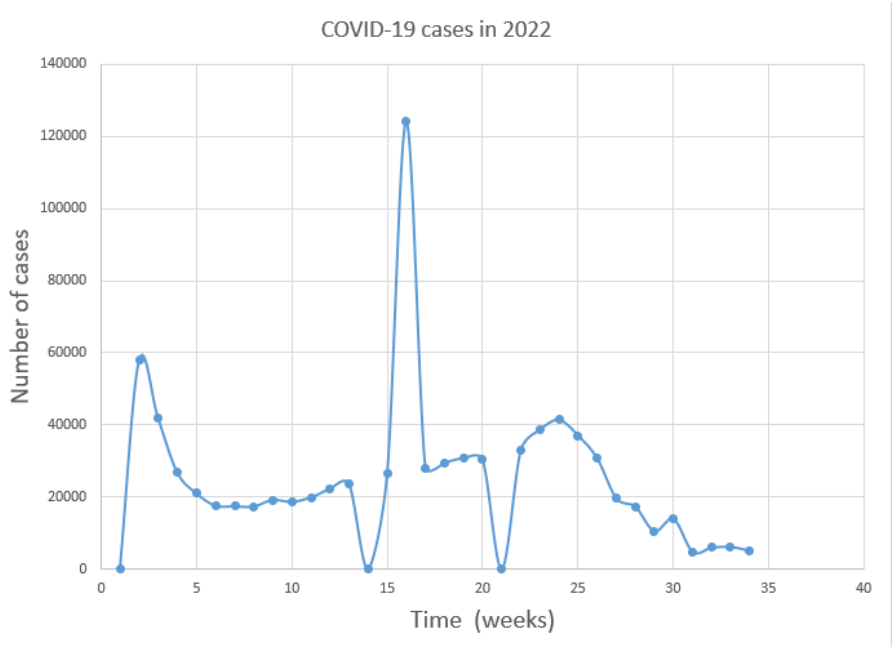

Figure 7.4: COVID-19 data set 2022 (number of cases)

7.2 Simulation results

7.2.1 Influenza model solution

We used the population age structure in the study of Dina Mistry mentioned previously as the initial condition (Table 7.5) and assumed that there were 1,000 latent patients and 1,000 infectious patients in each age group.

Figure 7.5 shows the effect of influenza vaccination, which reduces the peak number of infections by one-third compared to not using the vaccine at all.

Figure 7.6 shows the distribution of the total number of infections in each age group within one year. Since the vaccine coverage rate shows an upward trend with age, and the increase is large, it can be seen that people in older age groups are better protected by the vaccine (the gap between the blue column and the orange column is large). Figure 7.7 shows the protective effect of the vaccine in the form of proportion. It can be seen that with the increase of age, the proportion of cases reduced by the use of vaccines increases, and in the age group of 71-80, the number of cases has even decreased by more than 35%. At the same time, we

Parameter	Description	Value	Source
τ	Vaccine effectiveness is the same for all ages	95%	[20]
k_1	Age 1-10 vaccine coverage	37.6%	
k_2	Age 11-20 vaccine coverage	37.6%	
k_3	Age 21-30 vaccine coverage	37.6%	
k_4	Age 31-40 vaccine coverage	48.5%	
k_5	Age 41-50 vaccine coverage	48.5%	
k_6	Age 51-60 vaccine coverage	62.9%	
k_7	Age 61-70 vaccine coverage	71%	
k_8	Age 71-80 vaccine coverage	79.1%	
k_9	Age 80+ vaccine coverage	79.1%	
μ	Birth and death rate (weeks)	$\frac{0.0121}{52}$	[2]
ϵ	Immunity period	$\frac{1}{34}$	[19]
β_{ij}	Effective contact rate between age classes	β_{ij}	By calcualtion
β_1	Seasonality strength	0.1	By assumptions
N	Population	$26,955,026$	[10]
α	Incubation period	$\frac{7}{7.5}$	[4]
δ	Infection period	$\frac{7}{10}$	[4]
m	Time of vaccine becomes available	$(0, 52]$	By assumptions
v	Vaccine effective duration	$1/26$	[5]

Table 7.4: Parameter Descriptions and Values of COVID-19

also noticed that in the effective contact rate matrix heat map, the young group presents a higher risk of disease transmission, which is determined by their living habits and social contacts (the color of the cells aged 1-20 in the heat map is the brightest, which means that their transmission risk is the highest). However, this age group is not protected by the vaccine very much, so more consideration should be given to promoting vaccines among young people, so as to achieve a better effect of blocking the spread of influenza.

Table 7.5: Age structure of the Australian population

Age class	Prop	Population
1	0.064064	1,726,850.26
2	0.064771	1,745,901.66
3	0.065723	1,771,568.12
4	0.066660	1,796,811.22
5	0.067690	1,824,594.50
6	0.070227	1,892,967.85
7	0.068377	1,843,116.70
8	0.072332	1,949,698.67
9	0.073525	1,981,874.36
10	0.071450	1,925,937.35
11	0.068562	1,848,091.23
12	0.060884	1,641,118.98
13	0.055808	1,504,319.37
14	0.041838	1,127,736.79
15	0.031980	862,022.74
16	0.024357	656,532.26
17	0.015500	417,807.69
18	0.016252	438,076.26

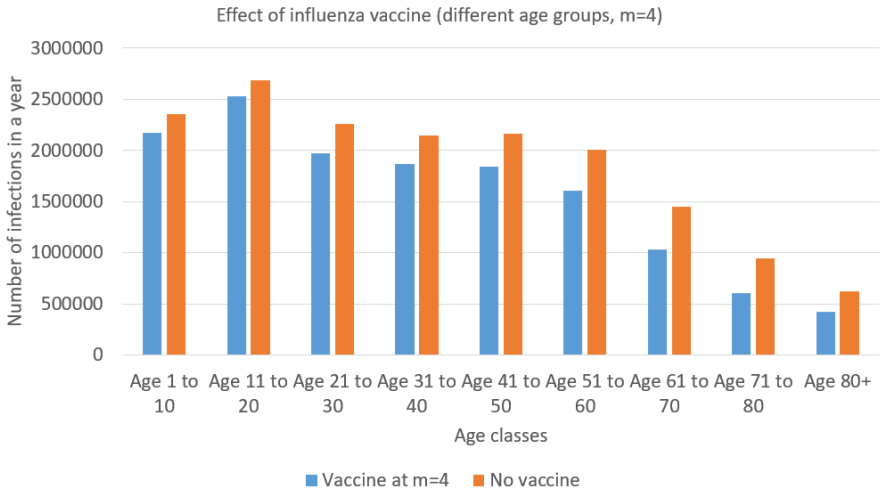

Figure 7.6: Effect of flu vaccine in each age group when vaccine becomes available at week 4 each year.

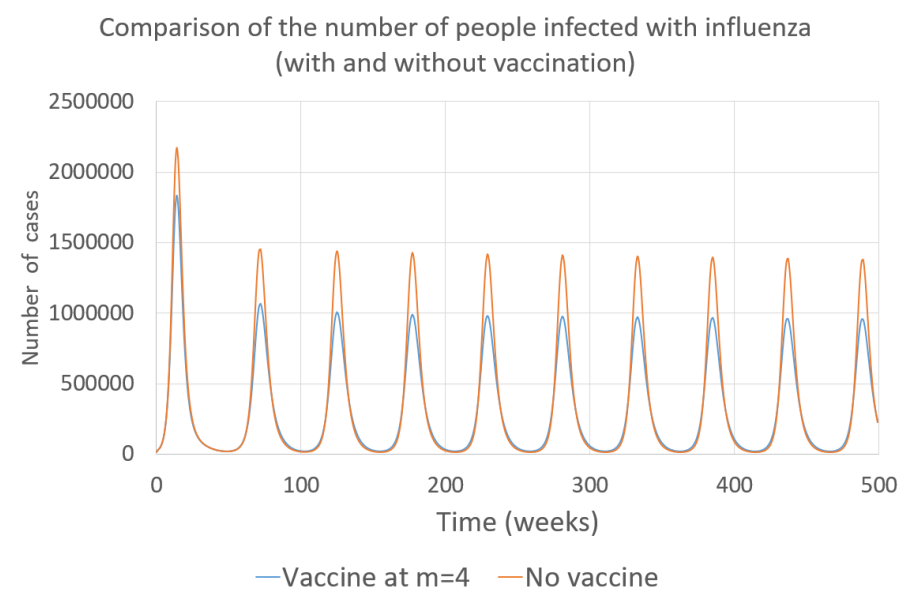

Figure 7.5: Flu vaccine effect

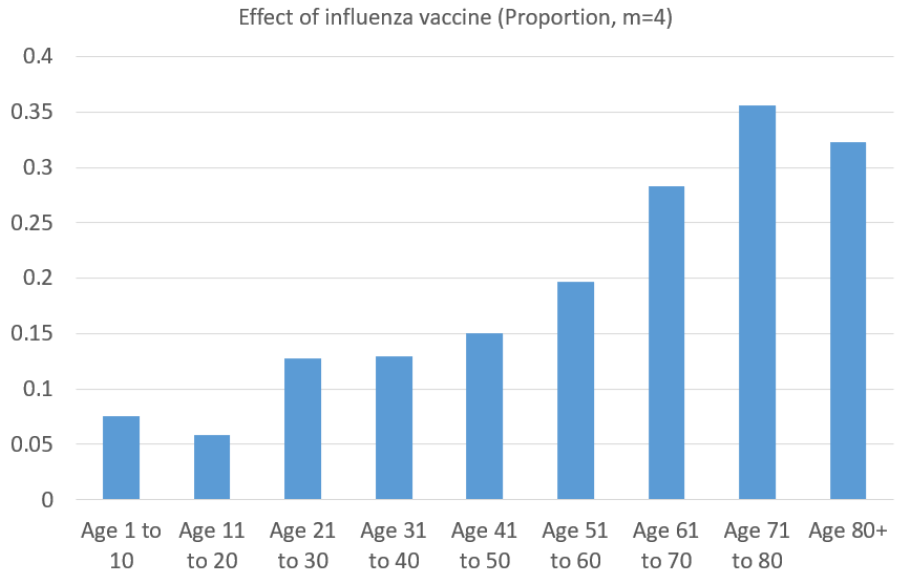

Figure 7.7: Effect of flu vaccine in proportion

7.2.2 COVID-19 model solution

Figures 7.8 to 7.10 show the numerical solution of the COVID-19 model and the age distribution of the number of infections. Since the seasonality of COVID-19 is completely based on assumptions, its trend is not specifically analyzed here.

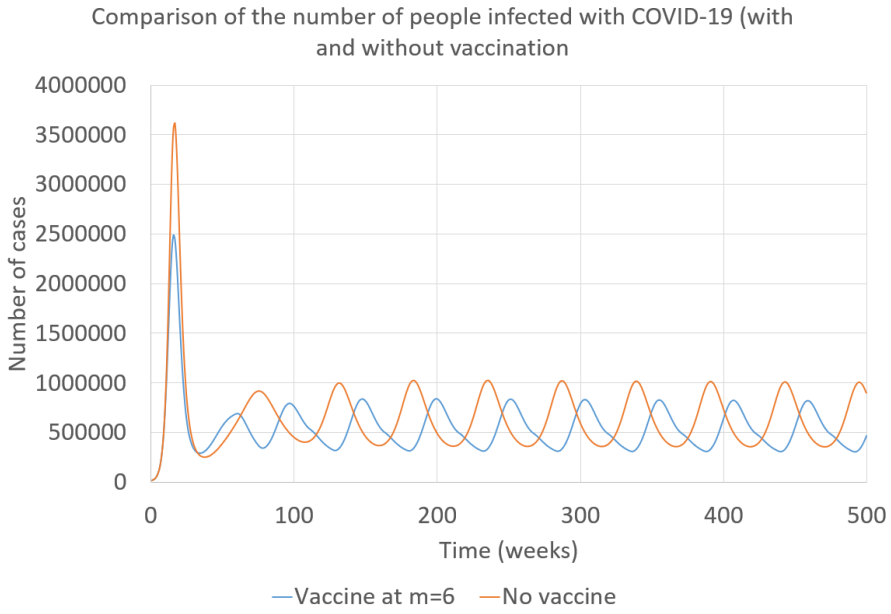

Figure 7.8: COVID-19 vaccine effect

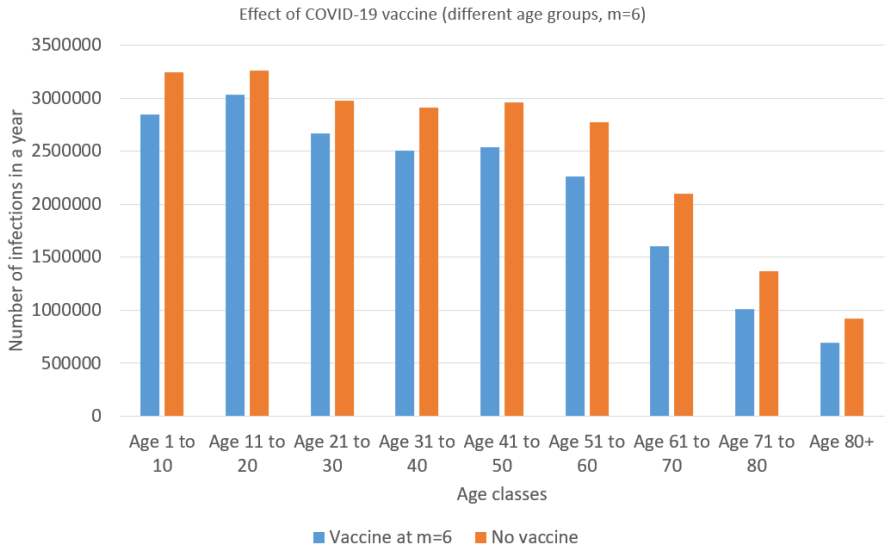

Figure 7.9: Effect of COVID-19 vaccine, m=6

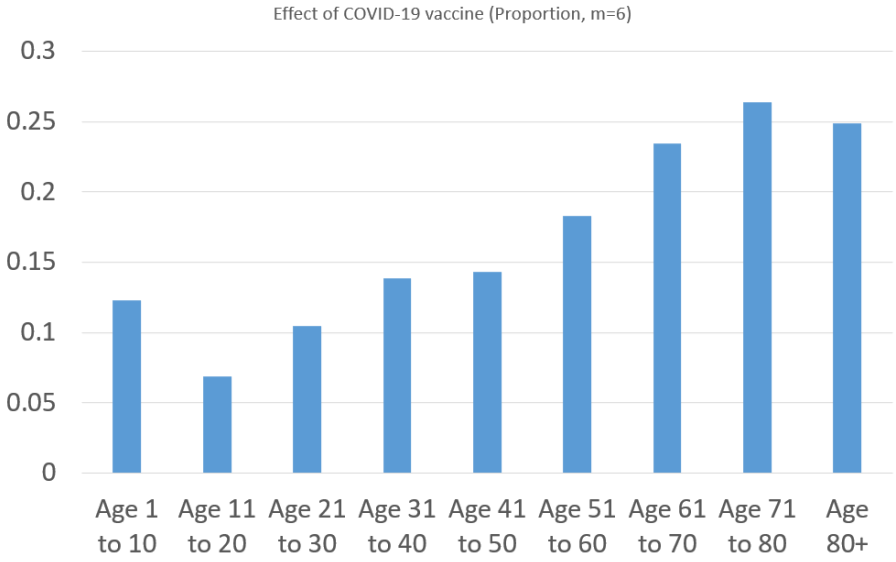

Figure 7.10: Effect of COVID-19 vaccine in proportion

7.3 Timing of vaccine intervention

Because both influenza and COVID-19 are seasonal under the assumptions of this study, and their peaks occur at different times, there is a need to consider when vaccination can most effectively reduce the number of cases.

7.3.1 Timing of flu vaccine

Figures 7.11 and 7.12 present the impact of different vaccine intervention timings (m values) on the number of infections. First, it can be observed from Figure 7.11 that whenever vaccination is started, it can significantly reduce the number of infected people. Through Figure 7.12, it is found that the impact of influenza vaccination on the number of infections reaches its peak (nearly 16%) when m=4. Therefore, it can be concluded that influenza vaccination starting at the end of January or early February every year can protect the population to the greatest extent.

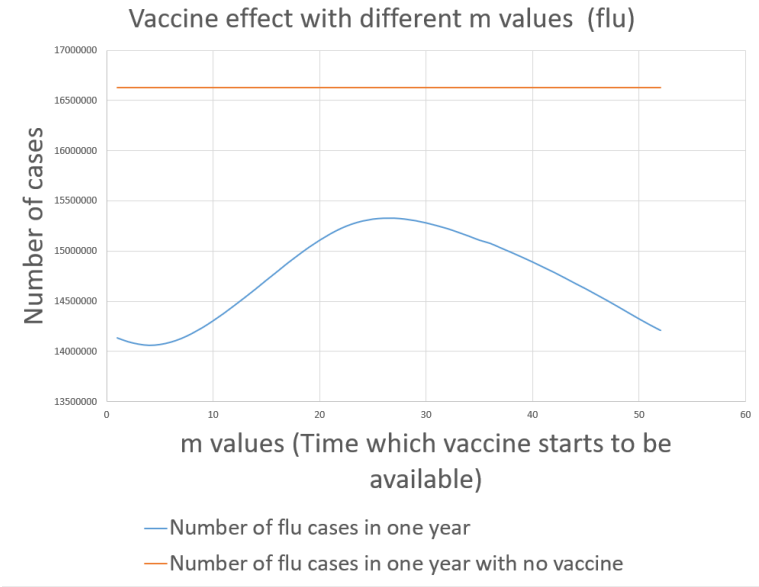

Figure 7.11: Flu vaccine effect with different m. (Vaccine becomes available from week m in each year)

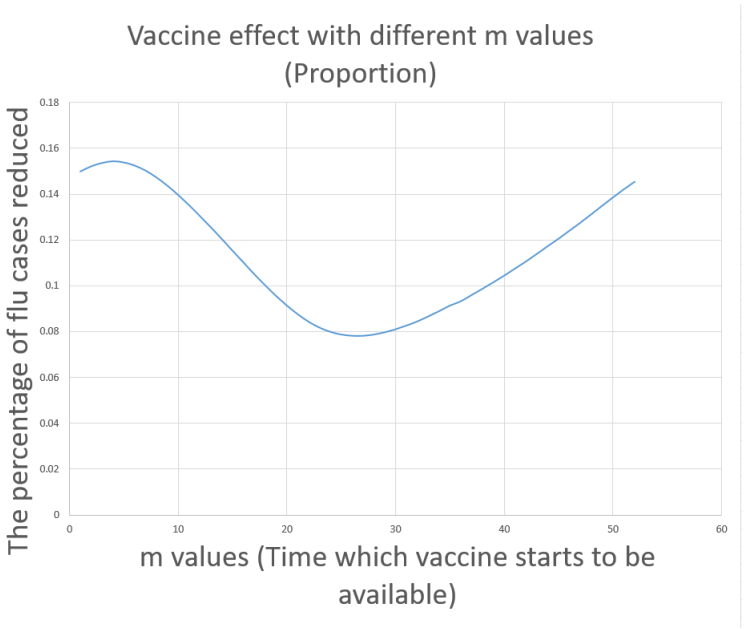

Figure 7.12: Flu vaccine effect with different m in proportion.(Vaccine becomes available from week m in each year)

7.3.2 Timing of COVID-19 vaccine

Similarly, regarding COVID-19, it can be concluded from Figures 7.13 and 7.14 that starting influenza vaccination in late February or early March each year (around m=6) can provide the greatest protection for the population.

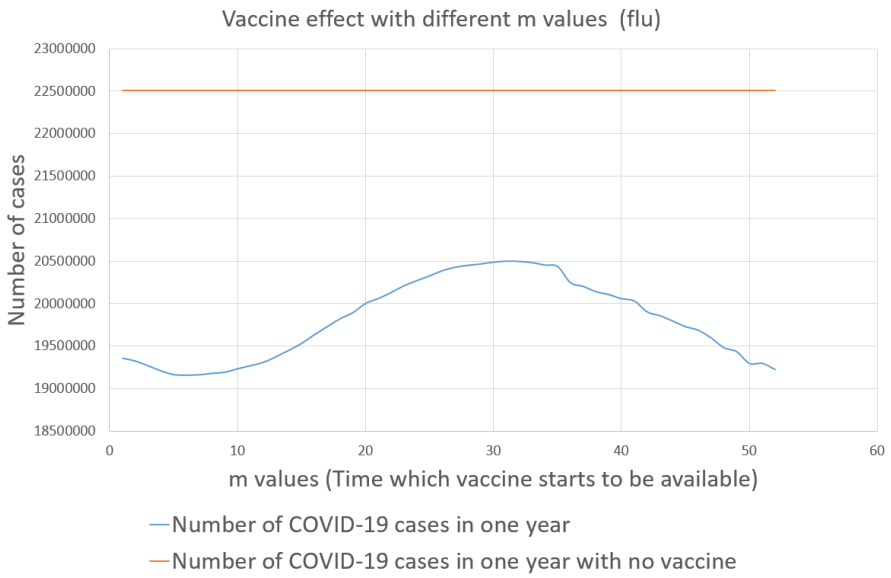

Figure 7.13: Flu vaccine effect with different m.(Vaccine becomes available from week m in each year)

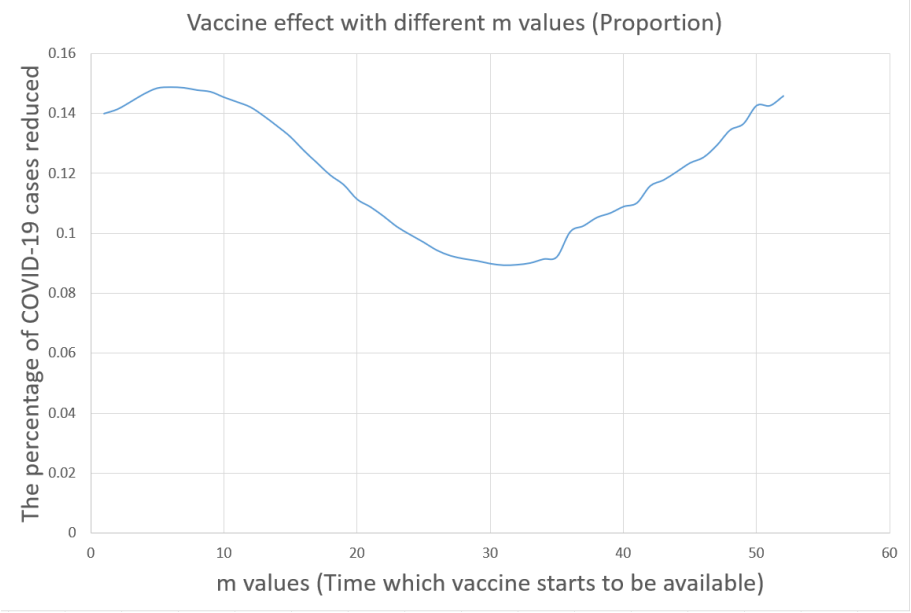

Figure 7.14: Flu vaccine effect with different m in proportion.(Vaccine becomes available from week m in each year)

7.3.3 Discussion on giving two vaccines at the same time

In fact, we have observed that vaccine penetration rates for influenza and COVID-19 are actually not high. This may be because people have become accustomed to facing these two diseases that have become normalized, so their willingness to get vaccinated is not strong. We hypothesized that if a person came to a vaccination site and could be vaccinated against both diseases, it would increase people's willingness to be vaccinated. On the other hand, there are also people who only care about one disease and ignore the prevention of another disease. If both vaccines are offered at the same time, this may help in filling the immune gap of this group of people. Of course, based on the analysis in previous chapters, we have also noticed that modifying the vaccination time will significantly affect the total number of infections. Therefore, if the negative effects of simultaneous vaccination are "acceptable", then such new measures can be considered to have certain feasibility.

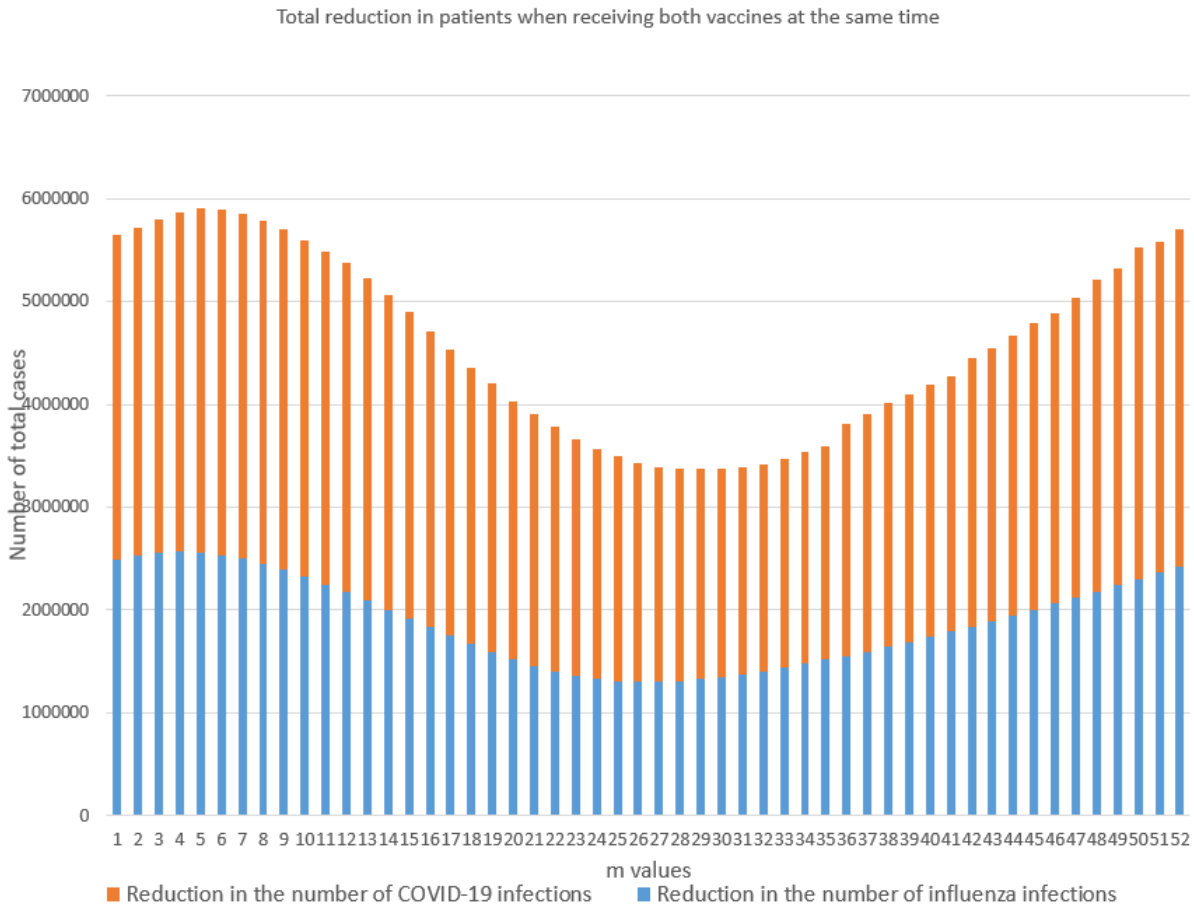

Figure 7.15: Total reduction of cases when vaccine at the same time

Figure 7.15 shows the total reduction in patients caused by starting vaccination at the same time at different time points. It can be observed that the best effect is achieved when vaccination is carried out at m=5. Compared with no vaccination at all, the total number of infections (COVID-19 + Influenza) in one year is reduced by 5902926 cases. The total reduction in patients caused by influenza vaccination at $m = 4$ and COVID-19 vaccination at $m = 6$ is 5918720.542. The difference is only 0.26%, so it can be considered that starting vaccination at the same time is feasible and will have a positive impact on the vaccination coverage rate.

Chapter 8

Future plan

After completing the initial simulation of the transmission dynamics of influenza and COVID-19 and evaluating the effects of vaccination interventions, the next phase of research will focus on further enhancing the model's precision and applicability, with emphasis on the following aspects:

Model Enhancement and Optimization:
The current model includes age structure and seasonality, but it also needs to account for more real-world factors, such as spatial heterogeneity. Future work will incorporate these factors and optimize parameter choices to improve model accuracy.

Dynamic Analysis of Coexisting Diseases:
In addition to influenza and COVID-19, this research could be extended to examine the coexistence and interaction of other seasonal respiratory diseases. For instance, the transmission of respiratory syncytial virus (RSV) could be included, exploring its interaction with public health strategies and the combined effects of administering multiple vaccines simultaneously.

Sensitivity Analysis of Vaccination Strategies:
The next step will focus on conducting sensitivity analysis on different vaccination strategies, investigating how factors like vaccine effectiveness, coverage, and timing impact the overall number of infections. Systematic adjustments to these parameters will provide more targeted recommendations for effective epidemic control.

Bibliography

[1] Nick Andrews, Elise Tessier, Julia Stowe, Charlotte Gower, Freja Kirsebom, Ruth Simmons, Eileen Gallagher, and Jamie Lopez Bernal. Duration of protection against mild and severe disease by covid-19 vaccines. *New England Journal of Medicine*, 386(4):340–350, 2022.

[2] Australian Bureau of Statistics. Births, australia. *ABS*, 2022. https://www.abs.gov.au/statistics/people/population/births-australia/2022.

[3] COVID-19 Data Australia. COVID-19 Data Australia, 2024. Accessed: 2024-10-24.

[4] Luca Ferretti, Alice Ledda, Chris Wymant, Lele Zhao, Virginia Ledda, Lucie Abeler-Dörner, Michelle Kendall, Anel Nurtay, Hao-Yuan Cheng, Ta-Chou Ng, Hsien-Ho Lin, Rob Hinch, Joanna Masel, A. Marm Kilpatrick, and Christophe Fraser. The timing of COVID-19 transmission. 2020. Preprint from medRxiv.

[5] Victoria Hall, Sarah Foulkes, Ferdinando Insalata, Peter Kirwan, Ayoub Saei, Ana Atti, Edgar Wellington, Jameel Khawam, Katie Munro, Michelle Cole, Caio Tranquillini, Andrew Taylor-Kerr, Nipunadi Hettiarachchi, Davina Calbraith, Noshin Sajedi, Iain Milligan, Yrene Themistocleous, Diane Corrigan, Lisa Cromey, Lesley Price, Sally Stewart, Elen de Lacy, Chris Norman, Ezra Linley, Ashley D. Otter, Amanda Semper, Jacqueline Hewson, Silvia D'Arcangelo, Meera Chand, Colin S. Brown, Tim Brooks, Jasmin Islam, Andre Charlett, and Susan Hopkins. Protection against sars-cov-2 after covid-19 vaccination and previous infection. *New England Journal of Medicine*, 386(13):1207–1220, 2022.

[6] J. A. P. Heesterbeek and K. Dietz. The concept of ro in epidemic theory.

[7] William O Kermack and Anderson G McKendrick. Contributions to the

mathematical theory of epidemics–i. 1927. *Bulletin of mathematical biology*, 53(1-2):33–55, 1991.

[8] Xiaoyue Liu, Jianping Huang, Changyu Li, Yingjie Zhao, Danfeng Wang, Zhongwei Huang, and Kehu Yang. The role of seasonality in the spread of covid-19 pandemic. *Environmental Research*, 195:110874, 2021.

[9] Dina Mistry, Maria Litvinova, Ana Pastore y Piontti, Matteo Chinazzi, Laura Fumanelli, Marcelo F. C. Gomes, Syed A. Haque, Quan-Hui Liu, Kunpeng Mu, Xinyue Xiong, M. Elizabeth Halloran, Ira M. Longini, Stefano Merler, Marco Ajelli, and Alessandro Vespignani. Inferring high-resolution human mixing patterns for disease modeling. *Nature Communications*, 12(1):323, 01 2021.

[10] Australian Bureau of Statistics. Population clock and pyramid, 2023.

[11] J.A. Quesada, A. López-Pineda, V.F. Gil-Guillén, J.M. Arriero-Marín, F. Gutiérrez, and C. Carratala-Munuera. Incubation period of covid-19: A systematic review and meta-analysis. *Revista Clínica Española (English Edition)*, 221(2):109–117, 2021.

[12] Jennifer M. Radin, Anthony W. Hawksworth, Christopher A. Myers, Michelle N. Ricketts, Erin A. Hansen, and Gary T. Brice. Influenza vaccine effectiveness: Maintained protection throughout the duration of influenza seasons 2010–2011 through 2013–2014. *Vaccine*, 34(33):3907–3912, 2016.

[13] Mohammad M. Sajadi, Parham Habibzadeh, Augustin Vintzileos, Shervin Shokouhi, Fernando Miralles-Wilhelm, and Anthony Amoroso. Temperature, Humidity, and Latitude Analysis to Estimate Potential Spread and Seasonality of Coronavirus Disease 2019 (COVID-19). *JAMA Network Open*, 3(6):e2011834–e2011834, 06 2020.

[14] S. G. SULLIVAN, K. S. CARVILLE, M. CHILVER, J. E. FIELDING, K. A. GRANT, H. KELLY, A. LEVY, N. P. STOCKS, S. S. TEMPONE, and A. K. REGAN. Pooled influenza vaccine effectiveness estimates for australia, 2012–2014. *Epidemiology and Infection*, 144(11):2317–2328, 2016.

[15] Julian Wei-Tze Tang and Tze Ping Loh. Influenza Seasonality. *Current Treatment Options in Infectious Diseases*, 8(4):343–367, 2016.

[16] Jeffrey P. Townsend, Hayley B. Hassler, April D. Lamb, Pratha Sah, Aia Alvarez Nishio, Cameron Nguyen, Alexandra D. Tew, Alison P. Galvani, and Alex Dornburg. Seasonality of endemic covid-19. *mBio*, 14(6):e01426–23, 2023.

[17] Timothy M. Uyeki, David S. Hui, Maria Zambon, David E. Wentworth, and Arnold S. Monto. Influenza. *The Lancet*, 400(10353):693–706, 2022.

[18] P. van den Driessche and James Watmough. Reproduction numbers and sub-threshold endemic equilibria for compartmental models of disease transmission. *Mathematical Biosciences*, 180(1):29–48, 2002.

[19] Yingcun Xia, Julia R. Gog, and Bryan T. Grenfell. Semiparametric Estimation of the Duration of Immunity from Infectious Disease Time Series: Influenza as a Case-Study. *Journal of the Royal Statistical Society Series C: Applied Statistics*, 54(3):659–672, 01 2005.

[20] Idan Yelin, Rachel Katz, Esma Herzel, Tamar Berman-Zilberstein, Amir Ben-Tov, Jacob Kuint, Sivan Gazit, Tal Patalon, Gabriel Chodick, and Roy Kishony. Associations of the BNT162b2 COVID-19 vaccine effectiveness with patient age and comorbidities. 2021. Preprint from medRxiv.